AD-A237 851

DOCUMENTATION PAGE

		1b. RESTRICTIVE MARKINGS
2b DECLASSIFICATION / DOWNGRADING SCHEDULE		3. DISTRIBUTION / AVAILABILITY OF REPORT APPROVED FOR PUBLIC RELEASE; DISTRIBUTION UNLIMITED

4 PERFORMING ORGANIZATION REPORT NUMBER(S)

5. MONITORING ORGANIZATION REPORT NUMBER(S)
AFOSR-TR- 91 0600

6a. NAME OF PERFORMING ORGANIZATION GEORGIA INSTITUTE OF TECHNOLOGY SCHOOL OF AEROSPACE ENGINEERING	6b OFFICE SYMBOL *(If applicable)*	7a. NAME OF MONITORING ORGANIZATION AIR FORCE OFFICE OF SCIENTIFIC RESEARCH
6c. ADDRESS (City, State, and ZIP Code) ATLANTA, GEORGIA 30332		7b ADDRESS (City, State, and ZIP Code) AFOSR/NA Bolling AFB DC 20332-644

8a. NAME OF FUNDING / SPONSORING ORGANIZATION AFOSR	8b OFFICE SYMBOL *(If applicable)* NA	9 PROCUREMENT INSTRUMENT IDENTIFICATION NUMBER AFOSR-89-0290

| 8c ADDRESS (City, State, and ZIP Code)
 AFOSR/NA
 Bolling AFB DC 20332-644 | 10 SOURCE OF FUNDING NUMBERS |

PROGRAM ELEMENT NO	PROJECT NO	TASK NO	WORK UNIT ACCESSION NO
61102F	2308	A1	

11. TITLE (include Security Classification)
"INVESTIGATION OF THE FLAME-ACOUSTIC WAVE INTERACTION DURING AXIAL SOLID ROCKET INSTABILITIES" (U)

12. PERSONAL AUTHOR(S)
B. T. ZINN, B. R. DANIEL, U. G. HEGDE.

13a. TYPE OF REPORT FINAL REPORT	13b TIME COVERED FROM 890301 TO 910228	14. DATE OF REPORT (Year, Month, Day) 910430	15 PAGE COUNT 46

16. SUPPLEMENTARY NOTATION

17		COSATI CODES	18 SUBJECT TERMS (Continue on reverse if necessary and identify by block number)
FIELD	GROUP	SUB-GROUP	SOLID PROPELLANT ROCKET, FLAME DRIVING, COMBUSTION ACOUSTICS, LONGITUDINAL INSTABILITY, FLOW TURNING LOSS

19 ABSTRACT (Continue on reverse if necessary and identify by block number)

(SEE BACK FOR ABSTRACT)

20 DISTRIBUTION / AVAILABILITY OF ABSTRACT ☒ UNCLASSIFIED/UNLIMITED ☐ SAME AS RPT ☐ DTIC USERS	21 ABSTRACT SECURITY CLASSIFICATION (U)
22a. NAME OF RESPONSIBLE INDIVIDUAL	22b TELEPHONE (Include Area Code)	22c OFFICE SYMBOL

DD Form 1473, JUN 86   *Previous editions are obsolete.*   SECURITY CLASSIFICATION OF THIS PAGE

UNCLASSIFIED

ABSTRACT

The primary objectives of this research program are: (1) to investigate the mechanisms responsible for the driving of axial instabilities by solid propellant flames, (2) to determine whether state-of-the-art theoretical models can predict the characteristics of the flame driving mechanisms, and (3) to investigate the effect of flow turning upon axial instabilities in solid propellant rocket motors. To attain the program's objectives, the response of diffusion flames, stabilized on the side wall of a duct, to imposed acoustic waves has been investigated by using flame radiation measurements and laser Doppler velocimetry (LDV). The flame radiation measurements revealed that the presence of an acoustic field produced space dependent oscillatory heat release rates which depend upon the characteristics of the flame and the excited acoustic field. Measurements of the flame radiation and velocity field both showed that at a given instant some sections of the flame drive the acoustic field while others damp it. The net effect of the flame upon the acoustic field depends on the relative magnitude of these driving and damping regions. The validity of a previously developed flame response model was investigated by comparing measured and predicted oscillatory velocity components in the flame region. Using measured values of the acoustic admittance of the burner, the flame shape, and the steady state temperature distribution in the flame region, the model was used to predict oscillatory vertical velocity distributions in the flame region. These were then compared to velocity distributions measured with an LDV system, showing good qualitative agreement. An experimental investigation was initiated into the effect of flow turning on an excited acoustic field. Failure of the experiments to show any effect larger than the inherent experimental errors of the measurement system prompted a theoretical investigation into the nature of the flow turning loss. This theoretical study revealed that because the flow turning loss is of first order in the mean flow Mach number, neglecting energy convection terms of the first order in mean Mach number in the original experimental procedure resulted in errors on the order of the flow turning loss. An improved experimental study into the flow turning losses in solid propellant rocket motors which includes the effects of terms proportional to the mean Mach number has been initiated.

1

AFOSR FINAL REPORT

on

INVESTIGATION OF THE FLAME - ACOUSTIC WAVE INTERACTION
DURING AXIAL SOLID ROCKET INSTABILITIES

Prepared for

Air Force Office of Scientific Research
·Aerospace Sciences Directorate
Bolling Air Force Base

Principle Investigators

Ben T. Zinn
Brady R. Daniel

School of Aerospace Engineering
Georgia Institute of Technology
Atlanta, GA 30332

Approved for public release; distribution unlimited

Grant No. AFOSR-89-0290

91 ᵕ 11 070

ABSTRACT

The primary objectives of this research program are: (1) to investigate the mechanisms responsible for the driving of axial instabilities by solid propellant flames, (2) to determine whether state-of-the-art theoretical models can predict the characteristics of the flame driving mechanisms, and (3) to investigate the effect of flow turning upon axial instabilities in solid propellant rocket motors. To attain the program's objectives, the response of diffusion flames, stabilized on the side wall of a duct, to imposed acoustic waves has been investigated by using flame radiation measurements and laser Doppler velocimetry (LDV). The flame radiation measurements revealed that the presence of an acoustic field produced space dependent oscillatory heat release rates which depend upon the characteristics of the flame and the excited acoustic field. Measurements of the flame radiation and velocity field both showed that at a given instant some sections of the flame drive the acoustic field while others damp it. The net effect of the flame upon the acoustic field depends on the relative magnitude of these driving and damping regions. The validity of a previously developed flame response model was investigated by comparing measured and predicted oscillatory velocity components in the flame region. Using measured values of the acoustic admittance of the burner, the flame shape, and the steady state temperature distribution in the flame region, the model was used to predict oscillatory vertical velocity distributions in the flame region. These were then compared to velocity distributions measured with an LDV system, showing good qualitative agreement. An experimental investigation was initiated into the effect of flow turning on an excited acoustic field. Failure of the experiments to show any effect larger than the inherent experimental errors of the measurement system prompted a theoretical investigation into the nature of the flow turning loss. This theoretical study revealed that because the flow turning loss is of first order in the mean flow Mach number, neglecting energy convection terms of the first order in mean Mach number in the original experimental procedure resulted in errors on the order of the flow turning loss. An improved experimental study into the flow turning losses in solid propellant rocket motors which includes the effects of terms proportional to the mean Mach number has been initiated.

1

INTRODUCTION

This research program is concerned with the development of an understanding of the mechanisms responsible for the driving of axial instabilities in solid propellant rocket motors. The onset of combustion instabilities in rocket motors depends upon the relative magnitudes of the gain (i.e., driving) and loss (i.e., damping) mechanisms within the combustor which add and remove energy from the oscillations, respectively. The reduction or elimination of the onset of combustion instabilities in solid propellant rocket motors requires identification of the processes which add or remove energy from the oscillations, and the development of an understanding of the mechanisms which control these processes. At present, it is generally recognized that the response of the solid propellant combustion process to the flow oscillations is responsible for providing the energy required for the initiation and maintenance of instabilities inside rocket motors. On the other hand, nozzle damping, viscous dissipation, flow turning, among others are processes which damp rocket instabilities. This research program has been concerned with developing an understanding of the gas phase flame processes which contribute to driving the instabilities, and the damping provided by the flow turning process.

Actual solid propellant gas phase flames are believed to consist of complex combinations of premixed and diffusion flames. Specifically, it has been argued that premixed flames occur above the oxidizer particles (e.g., ammonium perchlorate) and that diffusion flames are stabilized above the interfaces between the oxidizer particles and the fuel binder. Since premixed and diffusion flames are expected to respond differently to acoustic excitation, this investigation has been divided into two parts. In the first part of the study, completed earlier under this program, the interaction of premixed flames with axial acoustic fields was investigated. The parts of the study described herein investigated the response of diffusion flames to excited axial acoustic fields which simulate axial instabilities in solid propellant rocket motors, and began an investigation into the acoustic damping provided by the flow turning process.

Since actual solid propellant flames cannot be used in these studies because of their extremely small dimensions, their smoky nature, and rapid burnout, other

2

flames which simulate, in some respects, solid propellant flames have been used. In the present investigation, the response of diffusion flames, stabilized on the bottom wall of a long duct, to the excitation of axial acoustic fields has been studied. As with the previously conducted premixed flame investigations, the diffusion flame studies consist of parallel experimental and theoretical investigations of the diffusion flame response. Specifically, this research program has been investigating:

(1) the effects of diffusion processes on the acoustic driving/damping characteristics of the gas phase flame stabilized on the side wall of a duct,

(2) the validity of state-of -the-art solid propellant combustion response models,

and

(3) the effect of the flow turning upon axial instabilities in solid propellant rocket motors.

During the investigation, the experimental study of the interaction of diffusion flames with axial acoustic fields has been completed. In addition, the validity of the previously developed theoretical model of a diffusion flame response to axial acoustic fields was checked by comparing its predictions with experimental data. Preliminary results from the flow turning study revealed a need for a better theoretical understanding of the process, stimulating a theoretical investigation of the problem. This investigation has suggested a new experimental approach for investigating the effects of the flow turning upon axial acoustic fields, leading to the initiation of a new experimental study of the problem. Also, a simple computational model has been constructed that can be utilized to predict the approximate magnitudes of the various effects that are important to this type of flow field. This model will help in the analysis of future experimental data.

RESEARCH ACCOMPLISHMENTS

(A) Experimental diffusion flame studies:

The experimental phase of this program was conducted in the experimental setup shown in Fig. 1 which was developed earlier under this program. The interaction of three diffusion flames, stabilized on the bottom wall of a duct, with excited axial acoustic fields were investigated. The response of the diffusion flames to excited axial acoustic fields was studied by measuring steady and unsteady velocity components and distributions of C-H radiation from the flame using laser Doppler velocimetry and photomultipliers. In addition, pressure transducers were use to characterize the excited acoustic fields.

In a rocket motor, the interactions between unsteady solid propellant flames and the local flow oscillations involve complex fluid mechanical, heat transfer, and chemical processes. These interactions occur near the lateral boundaries of the motor cavity and they produce vertical velocity oscillations $v'(y)$ at and near the propellant surface in a direction normal to the direction of the axial oscillations in the core flow. These normal velocity oscillations act as lateral pistons which periodically compress the core flow, thus providing the energy required for initiating and maintaining the core flow oscillations. Specifically, if

$$I_v(y_i) = \int_L \int_T p' \, \text{Real}(v'(y_i)) \, dt \, dx \quad > 0 \qquad (1)$$

where p', L, T, and y_i are the local pressure oscillation, a relevant axial integration distance, the period of the oscillation, and the height above the flame, respectively, then these normal velocity oscillations pump acoustic energy into the core flow oscillations. Thus, if I_v increases with y in a given flame region, then the flame tends to drive the acoustic oscillation in this region, and vice versa.

The velocity measurements were conducted by using an existing LDV system, which had been also used for the premixed flame study. A typical measured time dependence of the normal velocity component a point in the flame is presented in Fig. 2. The variations of I_v in the vertical direction for two different driving frequencies measured at a pressure antinode are presented in Figs. 3 and 4. Figure 3

4

shows that I_v increases continually up to $0.55y_f$ (y_f is the flame height) and that it decreases subsequently. Based upon the above discussion, this result indicates that when the flame is subject to a 300 Hz. acoustic oscillation, the lower (where I_v increases) and upper (where I_v decreases) sections of the flame drive and damp the oscillation, respectively. The overall driving/damping of the flame depends upon the net effect of these two regions. Since $I_v(y_f) > I_v(y=0)$, the net effect of the flame is to drive the acoustic field. In contrast to the driving and damping regions which exist in the flame when it is subjected to a 300 Hz. wave, Fig. 4 shows that I_v increases continually along the whole length of the flame when the flame interacts with a 400 Hz. acoustic field, indicating that driving occurs throughout the flame region.

Flame radiation measurements are of interest because earlier studies[1] have shown that the radiation intensities from radicals such as C-H, C-C, and O-H are proportional to the reaction and heat release rates in the flame. Such radiation measurements were used in this study to determine the effect of the acoustic field upon the magnitude of the heat release rate and the phase relationship between the heat release and the local pressure oscillation. The latter is important because, as stated by Rayleigh's criterion[2], the phase difference between the oscillatory heat release rate and pressure oscillations determines whether the flame adds or removes energy from the acoustic waves. Expressed mathematically[3], a heat source, such as a flame, adds energy to the acoustic waves when the following inequality is satisfied:

$$\int_V |\,S_{p'q'}\,|\,\cos(\phi_{p'q'})\,dV \;>\; 0 \qquad\qquad (2)$$

where $|\,S_{p'q'}\,|$ and $\phi_{p'q'}$ are the magnitudes of the cross-spectrum between the pressure (p') and the oscillatory heat release rate (q') , and the phase difference between p' and q', respectively. The above integration is performed over the whole space where driving or damping by the flame occurs. In a flame region where the integrand is positive, driving of the acoustic waves occurs. This integrand is positive where p' and q' are in phase; that is, where $-90^o < \phi_{p'q'} < 90^o$. On the other hand, damping of the acoustic field by the flame occurs when p' and q' are out of phase; that is, when $-90^o > \phi_{p'q'} > 90^o$.

5

In the present study, C-H radiation measurements were carried out at different wave frequencies, different sections of the flame region, and with the flame located at different portions of the standing acoustic field; that is, at a pressure node and a pressure antinode. The radiation emission from the oscillatory flame was collected by the setup shown in Fig. 5. Paper shields containing slots at desired locations were placed on the optical windows of the test section in order to permit radiation measurements from specific regions of the flame. An appropriate bandpass filter (431 nm for C-H) was placed between the collecting lens and the photomultiplier to permit passage of only the wavelength of interest. The local pressure oscillations were measured with a transducer mounted on the wall above the flame. The studies revealed that:

(1) The autospectrum of the flame radiation exhibits a peak at the same frequency as the measured pressure autospectrum, and the amplitude of this peak is proportional to the amplitude of the excited pressure oscillation, see Figs. 6 and 7. These results indicate that the presence of an acoustic field results in a periodic heat release rate having the same frequency as the imposed acoustic field. Also, the magnitude of the oscillatory heat release process is proportional to the amplitude of the acoustic waves.

(2) Contrary to the results obtained with premixed flames which produced periodic radiation only when they were located away from an acoustic pressure node, the investigated diffusion flames produced oscillatory radiation when they were located next to acoustic pressure nodes and antinodes, see Fig. 8. This result indicates that the mechanisms which control the responses of the diffusion and premixed flames to acoustic oscillation are different. This result also suggests that the mechanism which controls the response of diffusion flames is responsive to both pressure and velocity oscillations.

(3) The phase difference between the total flame radiation and pressure oscillations depends upon both the frequency and the flame location relative to the standing acoustic wave, see Fig. 9. This figure shows that the flame adds energy to the acoustic waves at low frequencies. However, a transition from flame driving to damping occurs as the frequency increases beyond approximately 700 Hz. No oscillatory flame radiation was observed at frequencies higher than 800 Hz., suggesting that the investigated flames do not respond to these high frequencies, or that their response was too weak to be detected by the photomultiplier.

(4) An investigation of the variation of the flame to driving I_q (i.e., $I_q = \int_V | S_{p'q'} | \cos(\phi_{p'q'}) \, dV$) within the flame region along a distance normal to the burner surface showed that for a 300 Hz. acoustic wave the driving occurred at the lower part of the flame while damping occurred at its upper part, see Fig. 10. When the flame was exposed to a 400 Hz. wave, driving occurred along the entire length of the flame, as shown in Fig. 11. In these studies, the driving was determined by setting $dV = dy$ in the I_q integral, and using the radiation which passed through slits parallel to the x-axis to evaluate the integrand of the I_q integral. A comparison of these two results with those obtained using LDV velocity measurements (see Figs. 3 and 4), shows excellent qualitative agreement between the findings of the velocity and radiation measurements.

(5) The investigation of variation of the flame driving with axial distance showed that, for a 200 Hz. acoustic wave, the left and right sides of the flame drove and damped the acoustic waves, respectively, see Fig. 12. In this case, the integral describing I_q was determined by setting $dV = dx$ and using radiation which passed through vertical slits.

In an effort to better understand the processes which control the driving and damping by the flame, the phase differences between the pressure and radiation oscillations in different regions of the flame were investigated. Figure 13 shows that when the flame is located at a pressure node of the acoustic wave the phase differences between the radiation and pressure oscillations on the right side of the flame differ from those on the left side of the flame by almost 180° for all the investigated frequencies. On the other hand, Fig. 14 shows that when the flame is located at a pressure antinode, the phase differences between the radiation and pressure signals on the left and right sides of the flame are in the 120°-180° range. These results are consistent with the driving data presented in Fig. 12 and they indicate that, in most instances, when one side of the flame tends to drive the acoustic field, the other side of the flame tends to damp the acoustic oscillations. It is the relative magnitudes of the driving and damping provided by these two regions that determines whether the net effect of the flame is to drive or damp the acoustic motion.

The differences in the driving and damping tendencies of different regions of the investigated diffusion flames, which is discussed above, could have been caused

7

by the variations in the oscillatory velocity components in the flame region. In a steady, laminar, diffusion flame the flame location and reaction rate are primarily controlled by rates of convection and diffusion of the oxidizer, fuel, and other species into the flame sheets[1]. The presence of oscillatory flow velocities in the flame region is expected to modify the steady flame behavior. For example, when the flame is located at a pressure node, the oscillatory axial velocity vectors on both sides of the flame sheet are observed to be in phase, see Fig. 15. Consequently, they may increase and decrease the gas (i.e., primarily oxidizer) convection into the left and right sides of the flame, respectively. These, in turn, may increase and decrease the reaction rates of the left and right sides of the flame with respect to their mean reaction rates, respectively. Such behavior is expected to result in a 180° phase difference between the rates of heat addition of the left and right sides of the flame, which is consistent with the experimental findings of this study.

(B) Investigation of the validity of the flame response model:

An important objective of this research program was to examine the validity of the investigated flame response model which had been developed during the previous reporting period. This linear flame model requires the steady temperature distribution in the flame region, the flame shape, and the acoustic admittance of the burner surface as inputs. Using these input data, the model has been used to predict the distribution of the oscillatory velocity component normal to the burner. During the reporting period, the required input data were determined experimentally and the model was used to predict the velocity distributions within the investigated flames. These predictions were compared with corresponding experimental data. These efforts are briefly described in the remainder of this section.

The steady temperature distributions within the flame were performed by using a "Rayleigh scattering" technique. This technique has been widely used in flame temperature measurements[4] because it provides a non-intrusive way to measure the temperature with high spatial and temporal resolutions. A schematic of the utilized Rayleigh scattering temperature measurement setup is shown in Fig. 16. A 5 watt argon-ion laser was used as the light source. Scattered light from molecules was collected by a receiving system. A Hammamatsu R-268 photomultiplier was used to measure the intensity of the scattered light which

8

contains the temperature information. The relationship between the temperature and the measured scattered light for the flame configuration of this study can be expressed as[5]

$$T = T_{ref} * I_{ref} / I \tag{3}$$

where T_{ref} is a reference temperature (e.g., room temperature) and I_{ref} is the corresponding intensity of the scattered light. Thus, by measuring the Rayleigh scattering intensity, I, the temperature at any desired location can be obtained.

An important input parameter of the model is the Peclet number (Pe). In the present study this parameter was determined from a comparison of theoretically and experimentally determined flame heights. The experimental flame height was measured by cathetometer and the theoretical flame height was obtained from a solution of a modified Burke-Schumann model[6].

The acoustic admittance of the side wall burner assembly is another input required by the theoretical model. The admittance of the burner system was measured by the impedance tube technique[7]. The experimental setup used to determine the acoustic admittance of the burner is shown in Fig. 17. An acoustic standing wave of desired frequency was excited inside the duct by acoustic drivers. The interaction between the incident and reflected waves results in the formation of a standing wave pattern having successive maxima and minima along the duct, see Fig. 17. Using a traversing microphone to measure the amplitudes of the maxima and minima of the standing wave and the location of the first acoustic pressure minimum, it is possible to determine the acoustic admittance of the test sample[7].

Using the above described inputs, the model was used to predict the oscillatory vertical velocity distribution for different acoustic wave frequencies and amplitudes. Comparisons between predicted and measured distributions of the real part of the oscillatory vertical velocity, Re(v'), are presented in Figs. 18-20. Both the theoretical predictions and measured data show that Re(v') is space dependent and that it maximizes away from the flame region. The sharp peak in Re(v') predicted by the model is a result of the utilized flame sheet assumption. Figures 18 and 19 present comparisons of measured and predicted distributions of Re(v') for a 444 Hz. and a 300 Hz. acoustic wave, respectively, for the same amplitude of acoustic excitation. These results indicate that Re(v') is frequency dependent and that the

9

predicted and measured data are in qualitative agreement. Figure 20 presents a comparison of predicted and measured distribution of Re(v') for a 300 Hz. wave with an amplitude larger than that used in Fig. 19. These results show that a higher excitation amplitude causes a larger magnitude of Re(v') as expected. The model also predicts the same increase in the amplitude of Re(v') as observed experimentally.

(C) Flow turning studies:

An experimental investigation was begun in order to develop a greater understanding of the damping of combustion instabilities in solid rocket combustors due to 'flow turning'. A schematic of the experimental set-up is shown in Fig. 21. The steady state velocity field measured above the surface of the burner assembly is shown in Fig. 22. This figure shows that the region in which the added gases are turned in the direction of the core flow extends several centimeters above the burner surface. This is the region where 'flow turning' losses are expected to occur. Initial attempts, based upon a state-of-the-art theoretical approach[8], to measure the flow turning loss in cold flow failed to show any measurable effect. The classical acoustic energy flux, Real (p'u'), was measured and integrated over the surface of a control volume. Since no other sources or sinks of acoustic energy were present within the investigated control volume, any measured net loss of acoustic energy would represent the flow turning loss. This procedure was unable to measure any acoustic energy loss larger than experimental errors.

It was concluded that the inability to measure the flow turning loss may be due to one or more of the following:

(1) The experiment failed to account for the acoustic fluxes convected by the mean flow.

(2) The flow turning effect may be improperly predicted by Culick[9].

(3) The flow turning loss may be on the order of terms neglected in the experimental analysis.

To determine which of these factors could explain the experimental results, it was decided to rederive the expression for the flow turning loss by using a different theoretical approach from that used by Culick[9]. A one-dimensional acoustic stability

equation was developed from an energy balance approach, similar to that used by Cantrell and Hart[10].

The analysis was based on explicit considerations of mass, momentum, and acoustic energy fluxes at the control volume boundaries. It involved considerations of the first and second order perturbations of the acoustic quantities. The consideration of second order quantities is necessary for proper evaluation of terms of the order of the acoustic energy. Basically, the energy equation was expanded to second order in acoustic perturbations and the perturbed forms of the mass and momentum conservation equations were used to modify the energy equation. The original Cantrell and Hart analysis has been modified to include flow rotation effects. An expression for the acoustic growth rate α was derived which by careful manipulation was shown to be independent of any terms involving second order perturbations. The resulting stability equation is similar in form to Culick's 1-D result. This similarity to Culick's form of the acoustic stability equation is necessary for comparison of the results, and does not simplify interpretation of the terms. The resulting equation for a 2-D system is

$$-2\alpha < E^2 > = <[\ p'\ u'\ ]_0^L> + < [\frac{p'^2\ u_0}{\rho_o\ a^2}\ ]_0^L> + <[\ \rho_0\ u_0\ u'^2\ ]_0^L>$$

$$+< \int_0^L \frac{\rho_0\ u'}{H}\ [\ v'\ u_0\ ]_0^H\ dx > +< \int_0^L \frac{\rho_0\ u'}{H}\ [\ u'\ v_0]_0^H\ dx >$$

$$+< \int_0^L \frac{p'}{H}\ [\ \frac{m_b'}{\rho_0}\ ]_0^H\ dx > - < \int_0^L \frac{u'^2}{H}\ [\ m_{bo}\ ]_0^H\ dx > \qquad (4)$$

where α is the acoustic growth rate constant, E^2 is a term with units of energy, u and v represent velocity components in the axial and transverse directions, respectively, m_b is the mass flux out of the burning surface, and L and H are the length and height of the control volume. Values not evaluated at the walls are cross-duct averages. The equation is valid for constant height control volumes with no large variation in mean density ρ_0, no residual burning and no particles. It must be noted that the term E^2 does not represent the total acoustic energy of the system, but as a function of terms on the order of the perturbation squared, the term has a

11

growth rate of 2α. The lack of a simple physical interpretation of the E^2 term is an unfortunate but necessary consequence of the cancellation of any terms involving second order perturbations.

The last term on the right hand side of Eq. 4 corresponds to Culick's flow turning term. This 1-dimensional acoustic stability equation is more general than Culick's result in that it does not require the acoustic oscillations to be near a resonance of the system. Comparison shows that this result contains terms that are not found in Culick's result. The absence of these terms in Culick's result may be due to the inappropriate application of approximate boundary conditions. This work also confirms the results of Van Moorhem[11] which suggested that the flow turning effect is inherent to the 3-dimensional problem, and should not be added to the 3-dimensional stability equation as per Culick[12].

A numerical investigation was initiated to predict the nature and the relative magnitudes of the terms in the 1-dimensional acoustic stability equation (Eq. 4) derived in the above procedure. For this investigation the 2-dimensional acoustic equations including mean flow terms were averaged across a constant area duct of height H. The mean pressure p_0 and mean density ρ_0 were considered constant throughout the duct to the first order in Mach number. The isentropic value of the speed of sound was used. The acoustic perturbations were assumed to be harmonic in time at a given frequency ω, which represents a system that is neutrally stable. The equations were then integrated in a duct of length L. A schematic of the duct is shown in Fig. 23. The problem was simplified by setting the acoustic admittance of the injectors to 0, which allowed any terms proportional to the fluctuating part of the vertical velocity component v' to be neglected. Note that this is not a realistic assumption for walls made up of solid propellant, but is tolerable in this study because it helps to isolate the effect of the flow turning loss. The axial velocity component at the walls was set to zero, and because the inviscid equations were used, an infinitely thin boundary layer resulted. The results of the integration were used to evaluate each of the terms on the right hand side of Eq. 4. Terms involving integration along the axis were evaluated from 0 to x for each axial location. Neutral stability requires that the sum of these terms be constant along the duct when there is no net gain or loss of acoustic energy in the volume.

Results from two test cases are shown in Figs. 24-27. For these test cases the flow was assumed to be at room temperature. Figure 24 shows the acoustic pressure

12

amplitude and the phase of the pressure at a given axial location with respect to the phase of acoustic pressure at the head end of the duct for the case in which there is side injection at a local maximum of the pressure amplitude and no mean flow upstream of the side injection. The length of the side injector and the height of the duct are both 0.1 m. The injection is seen to have no discernable effect on the magnitude of the pressure and a relatively small effect on the phase of the pressure which is due to the mean axial velocity. The lack of any noticeable effect on the mode of the acoustic disturbance indicates that the effect of the flow turning, as well as the effects of the other terms of the acoustic stability equation, are relatively small. Figure 25 shows five terms relevant to the acoustic stability of the model and a graph of these terms and their sum as functions of axial location. Comparison of the graphed terms to the terms of Eq. 4 reveals that the stability of the system can be determined for an arbitrary section of the duct by subtracting the sum of the five terms at the left boundary of the volume from the sum of the five terms at the right boundary; ie., if the growth rate α is zero throughout the control volume, the value of 'term 6' must be constant along the length of the duct. This is expected because the oscillations in the duct were assumed neutrally stable in the computational model. In Figs. 26 and 27, the injection occurs at a local minima of the acoustic pressure amplitude. Comparison of Figs. 25 and 27 reveals that the magnitude of the flow turning loss depends on the axial location of the injection; eg., the flow turning loss is relatively higher when the injection occurs in the vicinity of an axial acoustic velocity maxima, and is relatively smaller when the injection occurs in the vicinity of an axial acoustic velocity minima. In the original experimental procedure, an attempt was made to measure the magnitude of the flow turning loss indirectly by measuring the deficit in the acoustic flux through the surface of the control volume. However, the convection of acoustic exergy by the mean flow was neglected as small with respect to the mean flow independent energy flux. The relative magnitudes of the terms in the acoustic stability equation reveal that the flow turning loss is of the order of these convective terms and therefore of the order of terms neglected in the original experimental procedure. The behavior of the terms predicted by the numerical model will be used to aid in the interpretation of data measured in an improved experimental procedure currently being initiated. This investigation will involve a more detailed study of the flow turning region

13

and the results will be analyzed using the acoustic stability equation derived above. The magnitude of the flow turning loss will be directly calculated from measured data, and then checked by indirect techniques. This new experimental procedure should ensure a more accurate determination of the magnitude of the flow turning loss and its importance to the stability of solid rocket motors.

SUMMARY

In the reported phase of this ongoing research program, theoretical and experimental investigations of the driving of axial acoustic fields by diffusion flames stabilized on the side wall of an acoustically excited duct were completed. In addition, initial results from an experimental study of the effects of flow turning upon axial acoustic instability failed to show expected results, which prompted a theoretical investigation into the nature of the flow turning loss.

Flame radiation measurements conducted during this study show that the excitation of acoustic waves produces space dependent oscillatory reaction and heat release rates within the investigated diffusion flames. At a given instant, some parts of the flame release energy in phase with the waves and, thus, drive the waves while other parts of the flame release energy out of phase with the pressure oscillations and, thus, damp the waves. This observation is consistent with LDV velocity data also measured during this study. The overall effect of the flame upon the acoustic wave depends upon the relative magnitudes of these "driving" and "damping" regions of the flame which add and remove energy from the acoustic wave. The results obtained in this study also suggest that both the pressure and velocity oscillations play an important role in the mechanism which controls the response of the diffusion flame to acoustic oscillations.

The velocity field measurements conducted during the diffusion flame study show that the interaction between the diffusion flames and the axial acoustic field produces an oscillatory transverse velocity component whose characteristics depend upon the spatial location, frequency, and amplitude of the acoustic wave. The predicted and measured distributions of $Re(v')$ are in good qualitative agreement.

Finally, preliminary results from an experimental investigation of the effect of flow turning upon axial combustion instabilities in solid rockets revealed the need for a more complete theoretical development of the flow turning losses. A theoretical investigation and a simple numerical model revealed that the original experimental procedure was inadequate for measuring the flow turning loss. A more detailed experimental procedure has been initiated using an acoustic stability equation derived during this theoretical investigation.

15

REFERENCES

1. Gavdon, A. G. and Wolfhard, H. G., "Flames: Their Structure, Radiation, and Temperature", 3rd Edition, Chapnanard Hall Ltd., 1970.

2. Lord Rayleigh, " The Theory of Sound", pp. 224-235 Vol. II, Dover Publications, 1945.

3. Putnam, A. A., "Non-Steady Flame Propagation", Chapter F, Pergamon Press, The Macmillan Co., N.Y., 1964.

4. Dibble, R. W. and Hollenbach, R. E., "Laser Rayleigh Thermometry in Turbulent Flames", 18th Symposium (International) on Combustion, 1980.

5. T. Chen, Ph.D. Thesis Proposal, G.I.T., 1989.

6. Hegde, U. G. and Zinn, B. T., "Interactions Between Axial Acoustic Waves and Sidewall Stabilized Diffusion Flames", 25th Joint Propulsion Conference, July, 1989, AIAA-89-2662.

7. Scott, R. A., Proceedings of the Physical Society, Vol. 58, pp. 253-264, 1946.

8. Zinn, B. T., Hegde, U. G., and Daniel, B. R., "Investigation of the Flame-Acoustic Wave Interaction During Axial Solid Rocket Instabilities", Proposal submitted to AFOSR in Oct., 1987.

9. Culick, F. E. C., "The Stability of One-Dimensional Motions in a Rocket Motor", Combustion Science and Technology, Vol. 7, 1973, pp 165 - 175.

10. Cantrell, R. H. and Hart, R. W., "Interactions Between Sound and Flow in Acoustic Cavities: Mass, Momentum, and Energy Considerations," Journal of the Acoustical Society of America, Vol. 36, No. 4, April 1964, pp 697 - 706.

11. Van MoorhemW. K., "Theoretical Basis of the Flow Turning Effect in Combustion Stability," Final Report, AFOSR Grant No. AFOSR78-3645, March 1980.

12. Culick, F. E. C., "Stability of Three-Dimensional Motions in a Combustion Chamber," Combustion Science and Technology, Vol. 10, pp. 109-124, 1975.

PROFESSIONAL INTERACTIONS

A. Professional Personnel:

Dr. Ben T. Zinn, Regent's Professor

Mr. Brady R. Daniel, Senior Research Engineer

Dr. Uday G. Hegde, Research Engineer

Dr. Tzengyuan Chen, Research Assistant

Mr. Lawrence M. Matta, Ph. D. Student

B. Publications:

1. Hegde, U. G. and Zinn, B. T., "Interaction Between Axial Acoustic Waves and Sidewall Stabilized Diffusion Flames", 25th Joint Propulsion Conference, July, 1989, AIAA-89-2662

2. Chen, T. Hegde, U. G., and Zinn, B. T., "Driving of Axial Acoustic Fields by Sidewall Stabilized Diffusion Flames", 26th JANNAF Combustion Meeting, Oct. 23-27, 1989

3. Chen, T. Hegde, U. G., and Zinn, B. T., "Driving of Axial Acoustic Fields by Sidewall Stabilized Diffusion Flames", 28th Aerospace Sciences Meeting, Reno, Nevada, Jan. 8-11, 1990, AIAA-90-0037

4. Sankar, S. V., Jagoda, J. I., and Zinn, B. T., "Oscillatory Velocity Response of Premixed Flat Flames Stabilized in Axial Acoustic Velocity Fields", Combustion and Flame, Vol. 80, No. 3 & 4, pp. 371-384, June 1990.

5. Chen, T. Hegde, U. G., Daniel, B. R., and Zinn, B. T., "Flame Driving of Axial Acoustic Fields: Comparison between Flame Radiation and Acoustic Intensity Measurements", AIAA Paper No. 90-3929, Oct. 22-24, 1990.

6. Chen, T., Jagoda, J. I., Zinn, B. T., and Daniel, B. R., "Measured and Predicted Responses of Diffusion Flames to Axial Acoustic Fields," AIAA Paper No. 91-0369, Jan 7-10, 1991.

C. Presentations:

1. "Flame-Acoustic Wave Interactions During Axial Solid Rocket Instabilities," Presented at the AFOSR Contractors Meeting, Ann Arbor, MI, June 20-25, 1989

17

2.   "Interaction Between Axial Acoustic Waves and Sidewall Stabilized Diffusion Flames", Presented at the AIAA/ASME/SAE/ASEE 25th Joint Propulsion Conference, July, 1989

3.   "Driving of Axial Acoustic Fields by Sidewall Stabilized Diffusion Flames", Presented at the 26th JANNAF Combustion Meeting, Pasedena, Ca., Oct. 23-27, 1989

4.   "Driving of Axial Acoustic Fields by Sidewall Stabilized Diffusion Flames", Presented at the 28th Aerospace Sciences Meeting, Reno, Nevada, Jan. 8-11, 1990

5.   "Flame Driving of Axial Acoustic Fields: Comparison between Flame Radiation and Acoustic Intensity Measurements", Presented at the AIAA 13th Aeroacoustics Conference, Tallahassee, FL, Oct. 22-24, 1990.

6.   "Predicted and Measured Responses of Diffusion Flames to Axial Acoustic Fields," paper presentation at the 27th JANNAF Combustion Meeting, Cheyenne, WY, Nov. 5-9, 1990.

7.   "Measured and Predicted Responses of Diffusion Flames to Axial Acoustic Fields," paper presented at the 29th Aerospace Sciences Meeting, Reno, Nevada, Jan. 7-10, 1991.
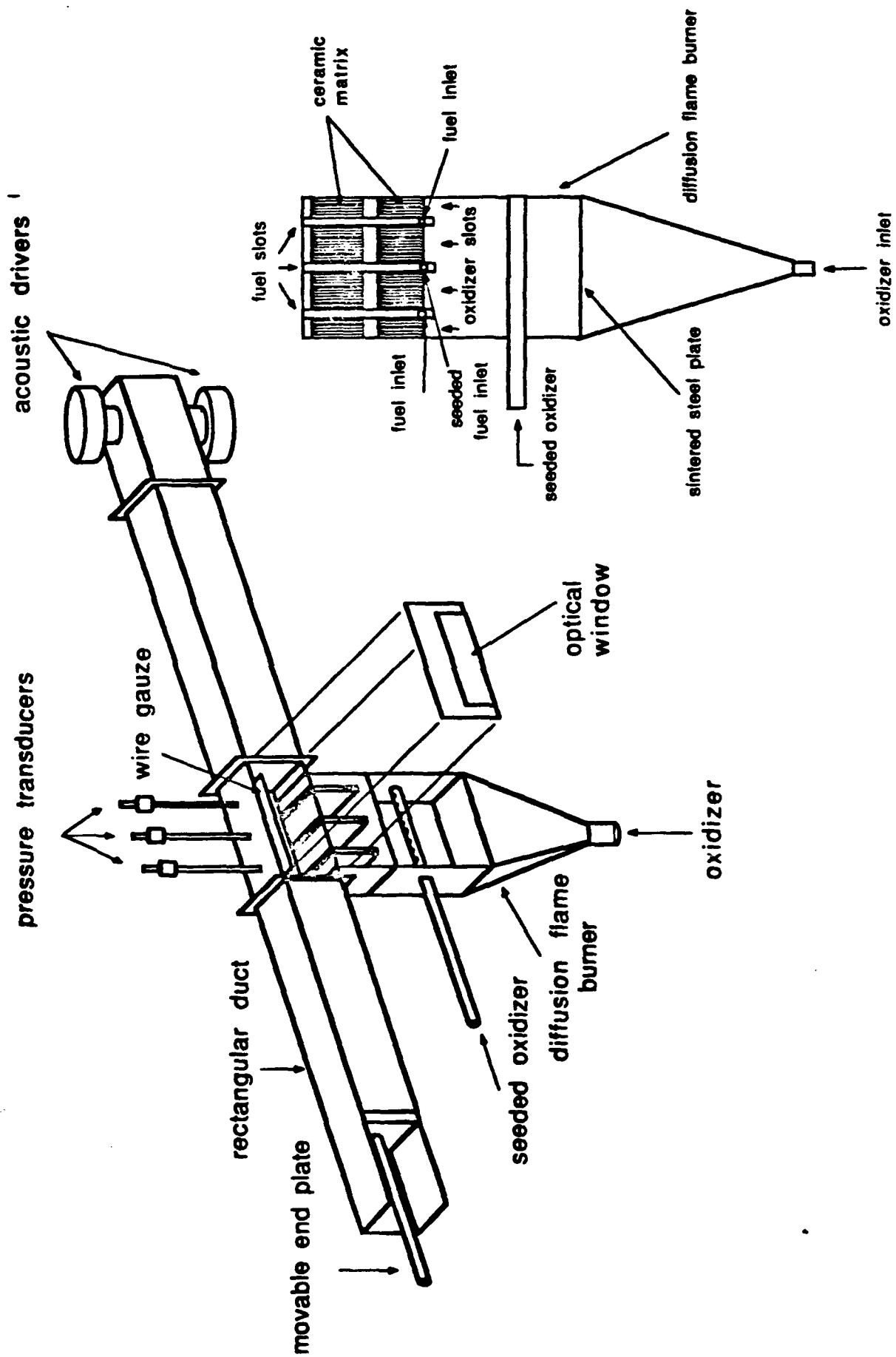
Figure 1. A Schematic of the Experimental setup
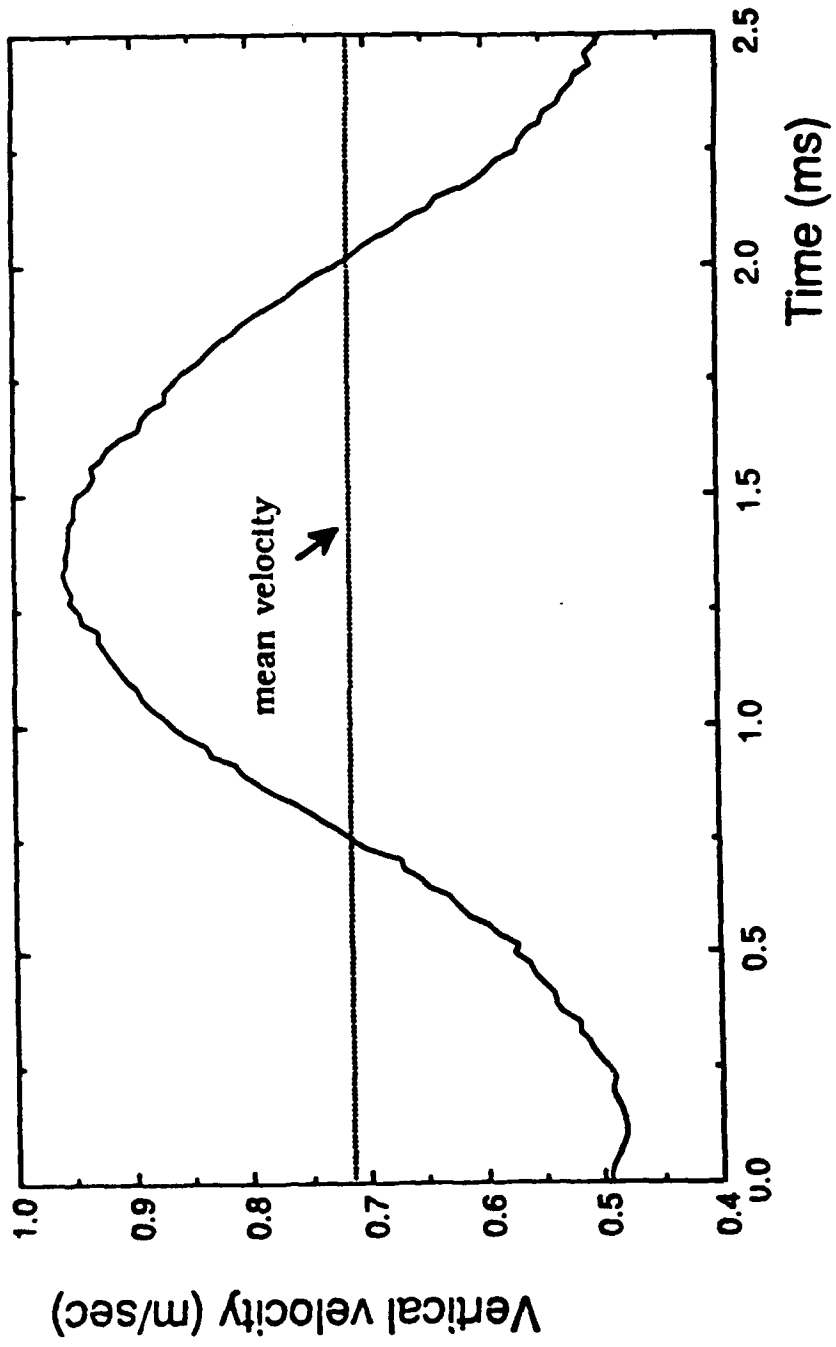
Figure 2. Typical Time Trace of the Vertical Velocity of a 400Hz. Oscillation at a Pressure Antinode.
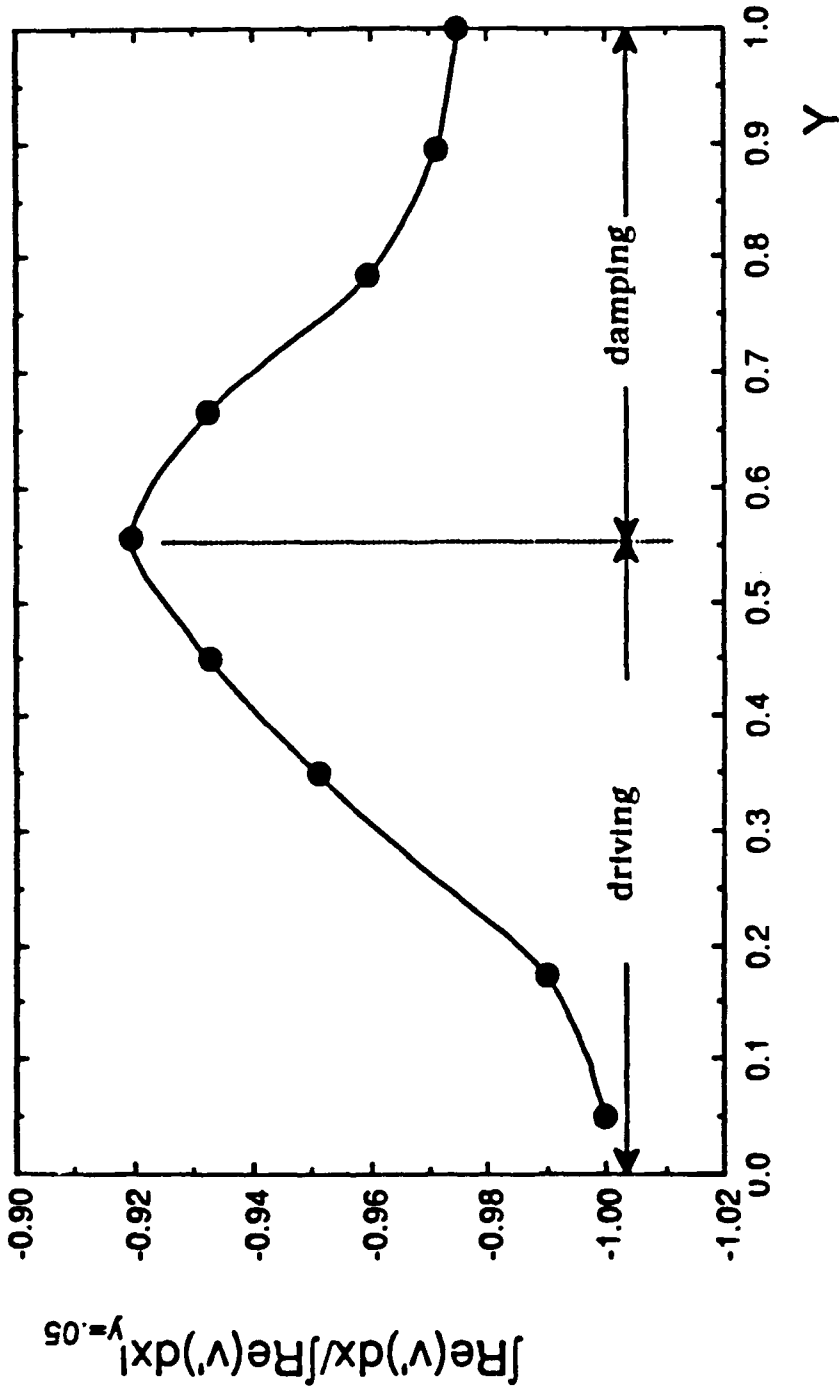
Figure 3. Measured Spatial Dependence of $\int$Re(v')dx along a Distance Normal to the Burner Surface of a Flame at a Pressure Antinode of a 300 Hz. Acoustic Wave.
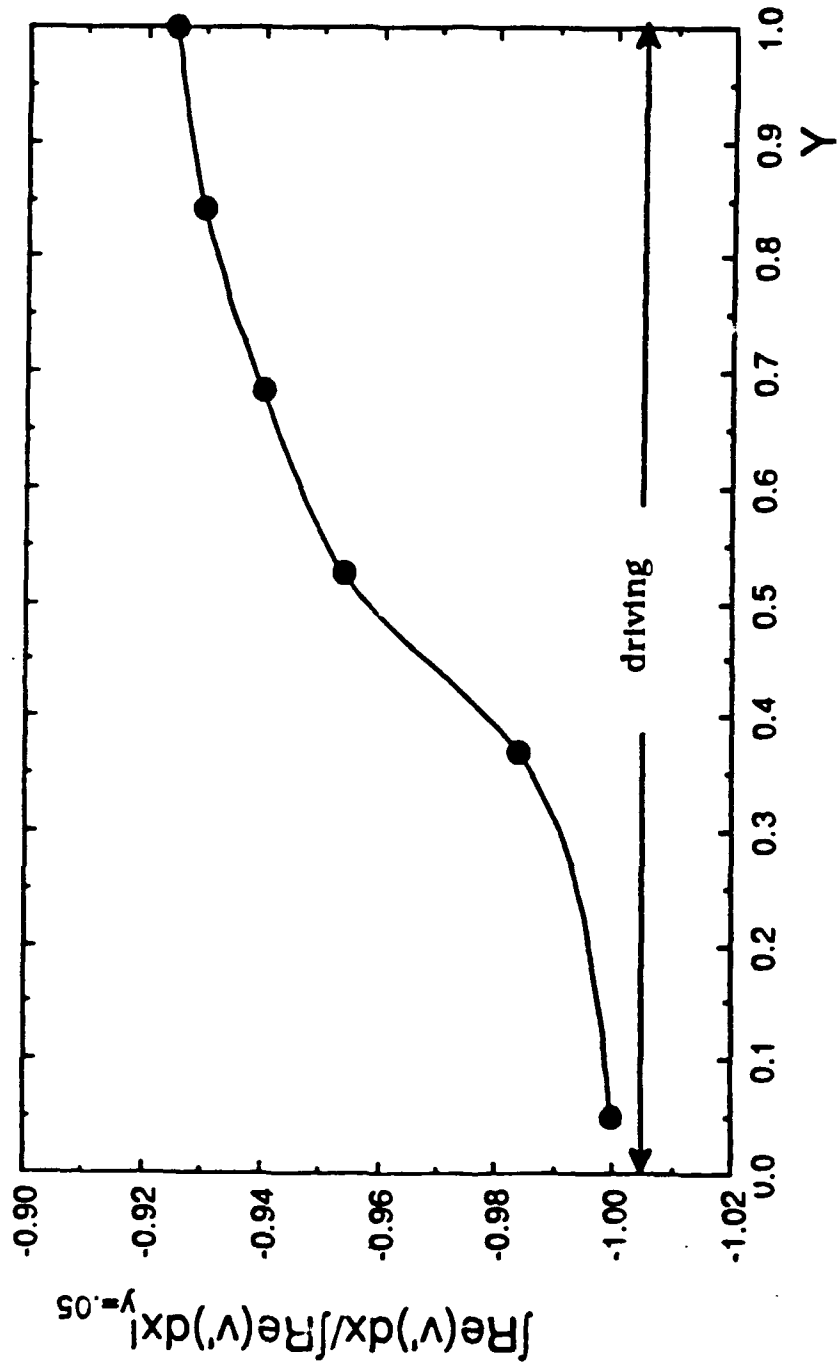
Figure 4. Measured Spatial Dependence of $\int Re(v')dx$ along a Distance Normal to the Burner Surface of a Flame at a Pressure Antinode of a 400 Hz. Acoustic Wave.
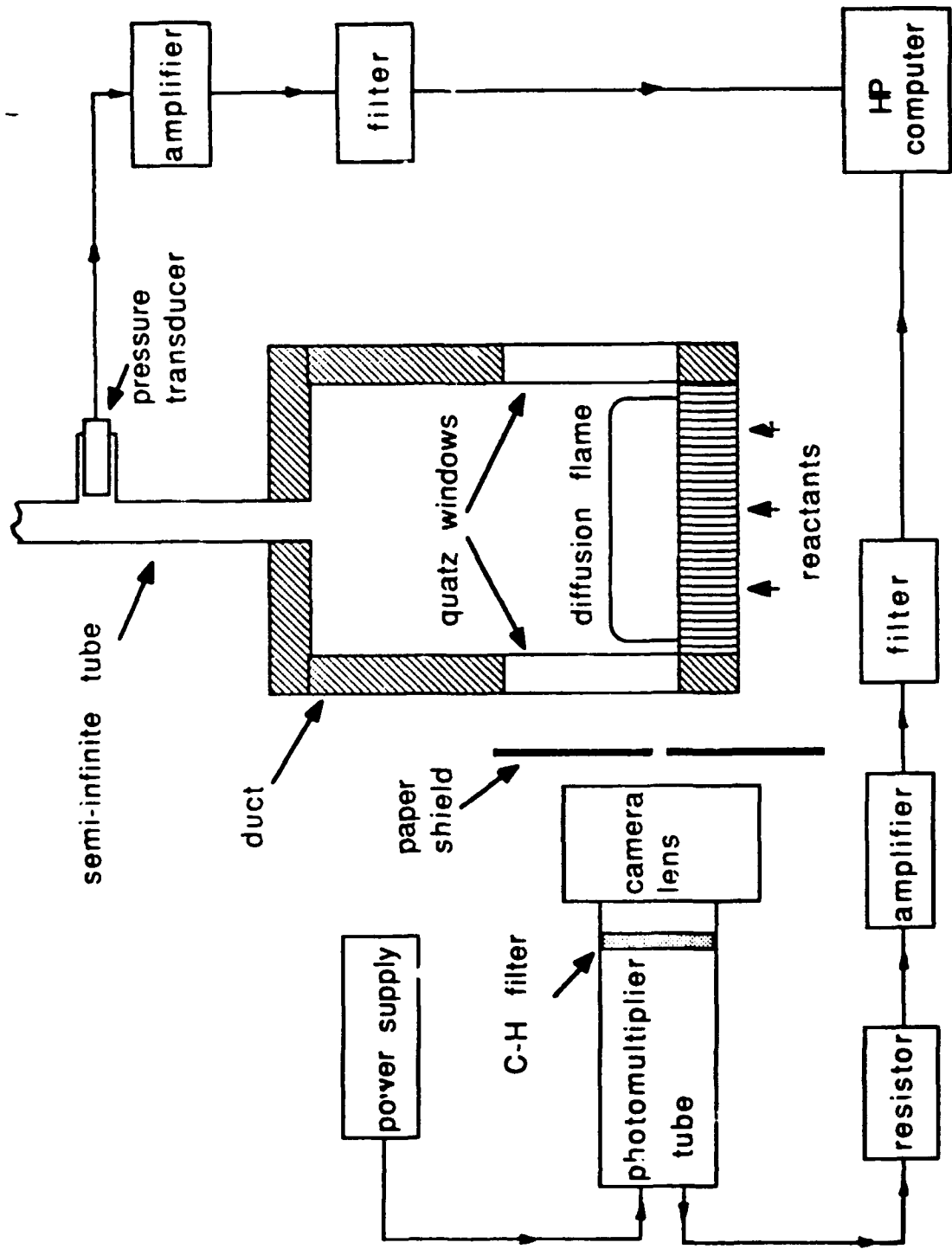
Figure 5. A Schematic of Flame Radiation Measurement Setup
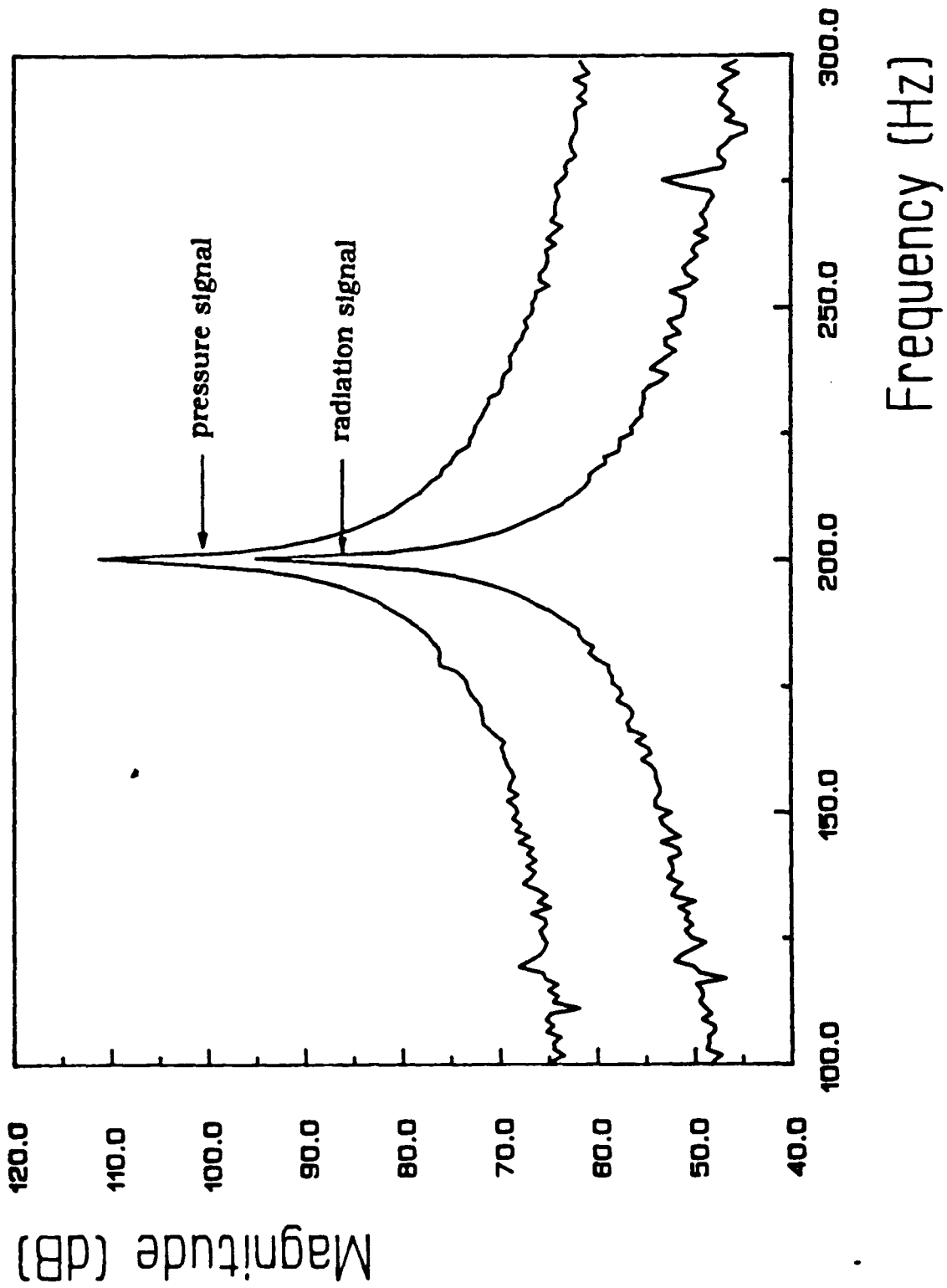
Figure 6. Autospetra of the Combustor Pressure and the Flame Radiation at a Driving Frequency of 200 Hz.
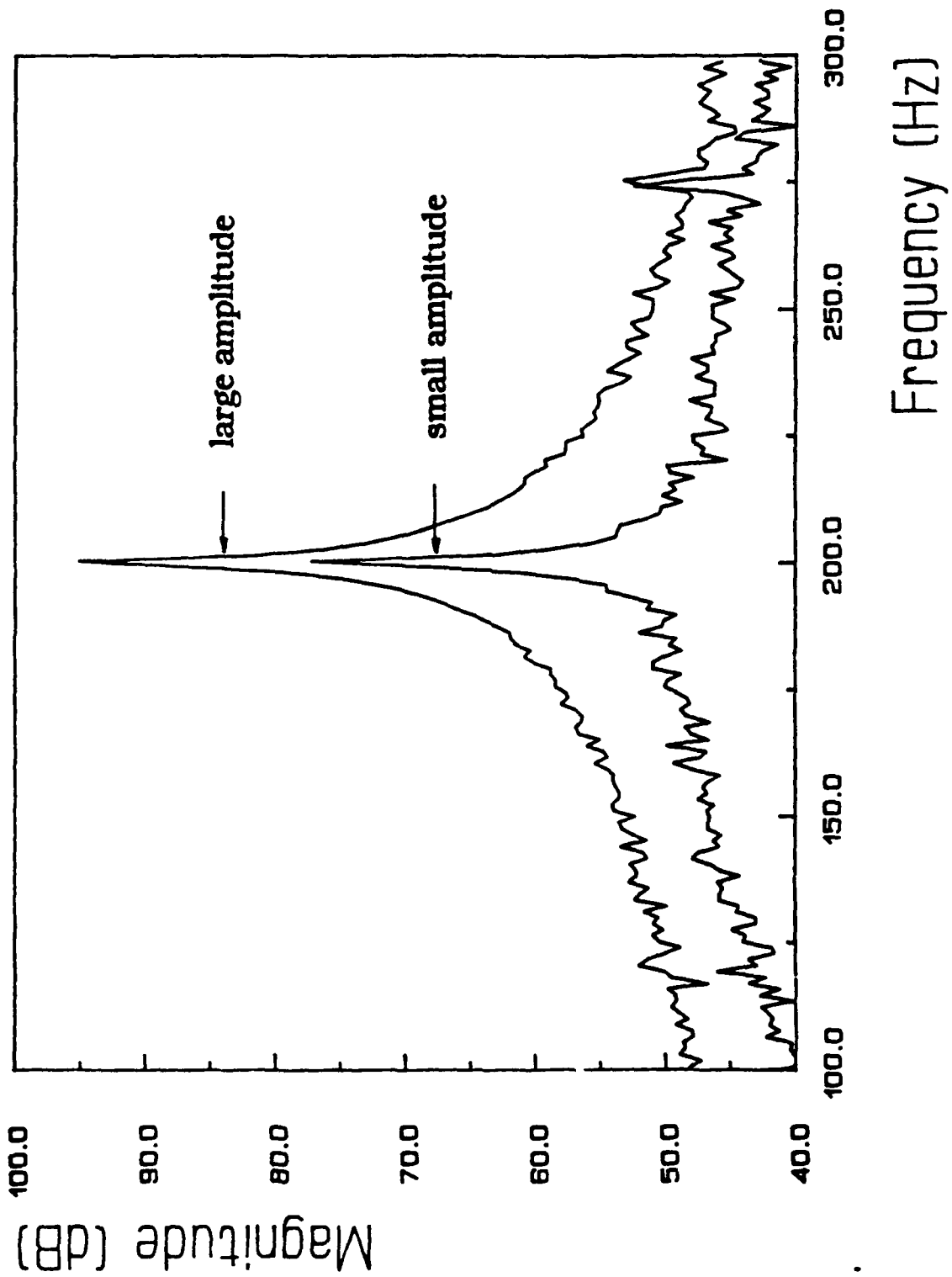
Figure 7. Autospectra of the Flame Radiation Measured with Large and Small Amplitude Excition.
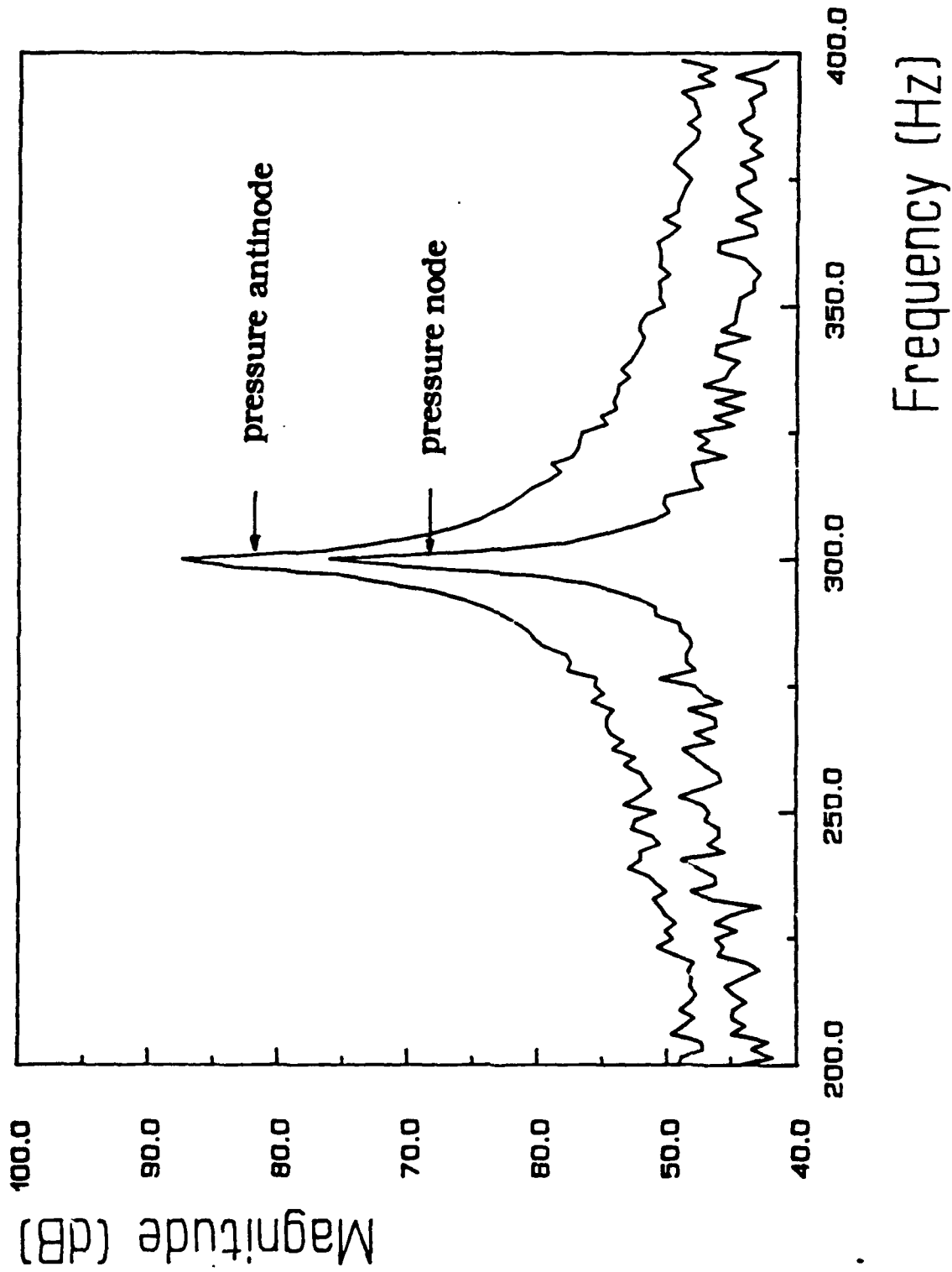
Figure 8. Autospectra of the Flame Radiation Measured with the Flame Positioned at a Pressure Node and a Pressure Antinode.
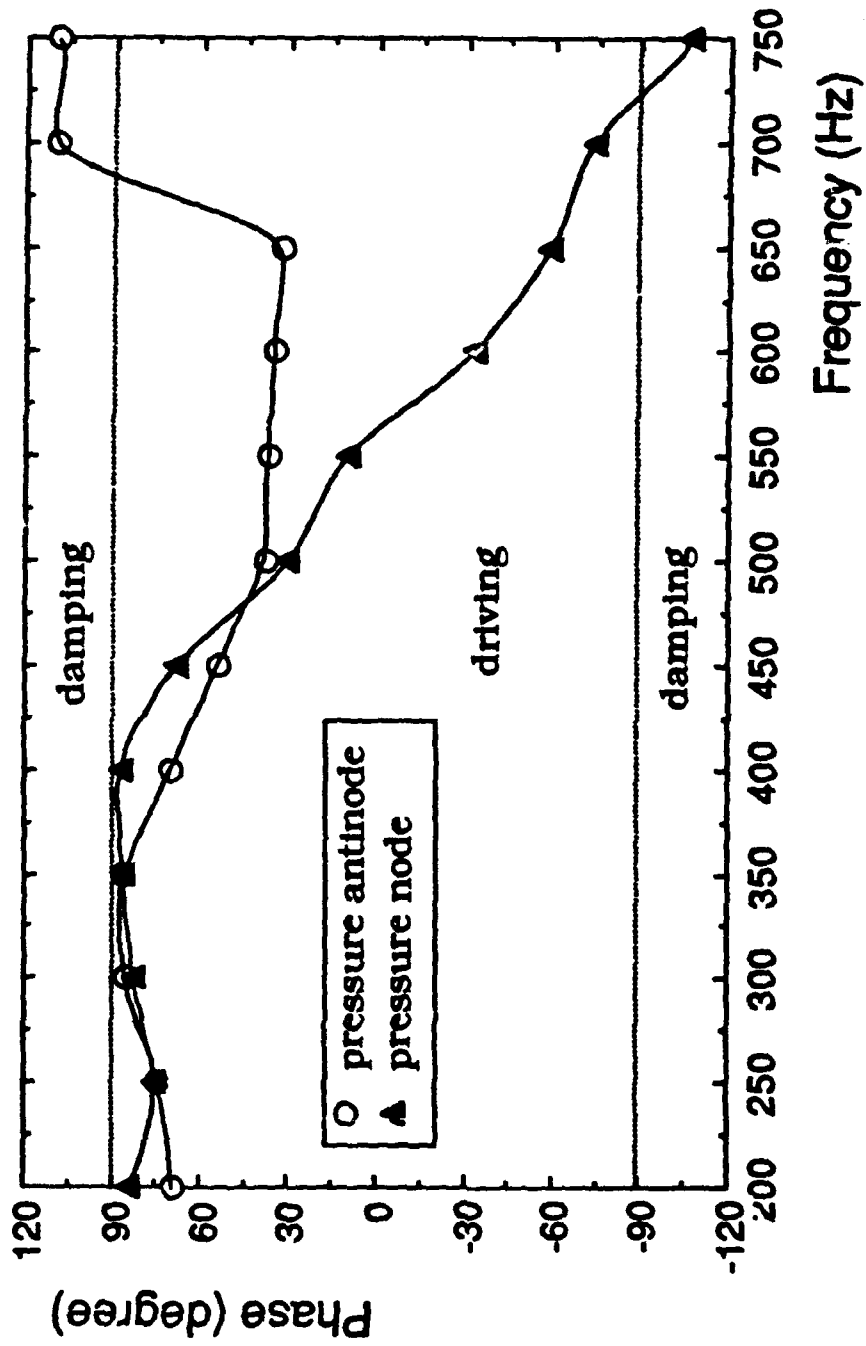
Figure 9. Phase Differences between the Radiation and Pressure Oscillations Measured with the Flame at a Pressure Antinode and a Pressure Node.
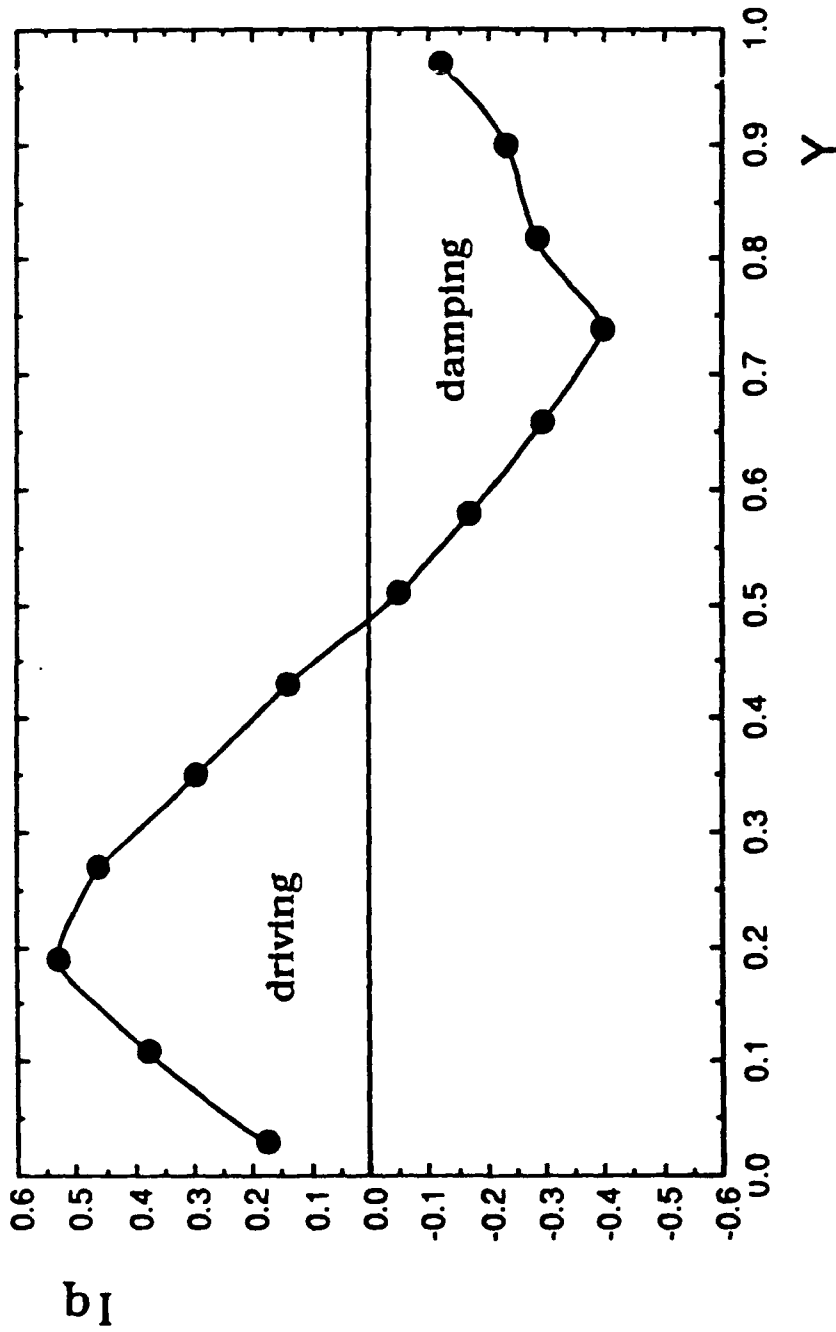
Figure 10. Variation of the Flame Driving/Damping along a Distance Normal to the Burner Surface of a Flame at a Pressure Antinode of a 300 Hz. Wave.
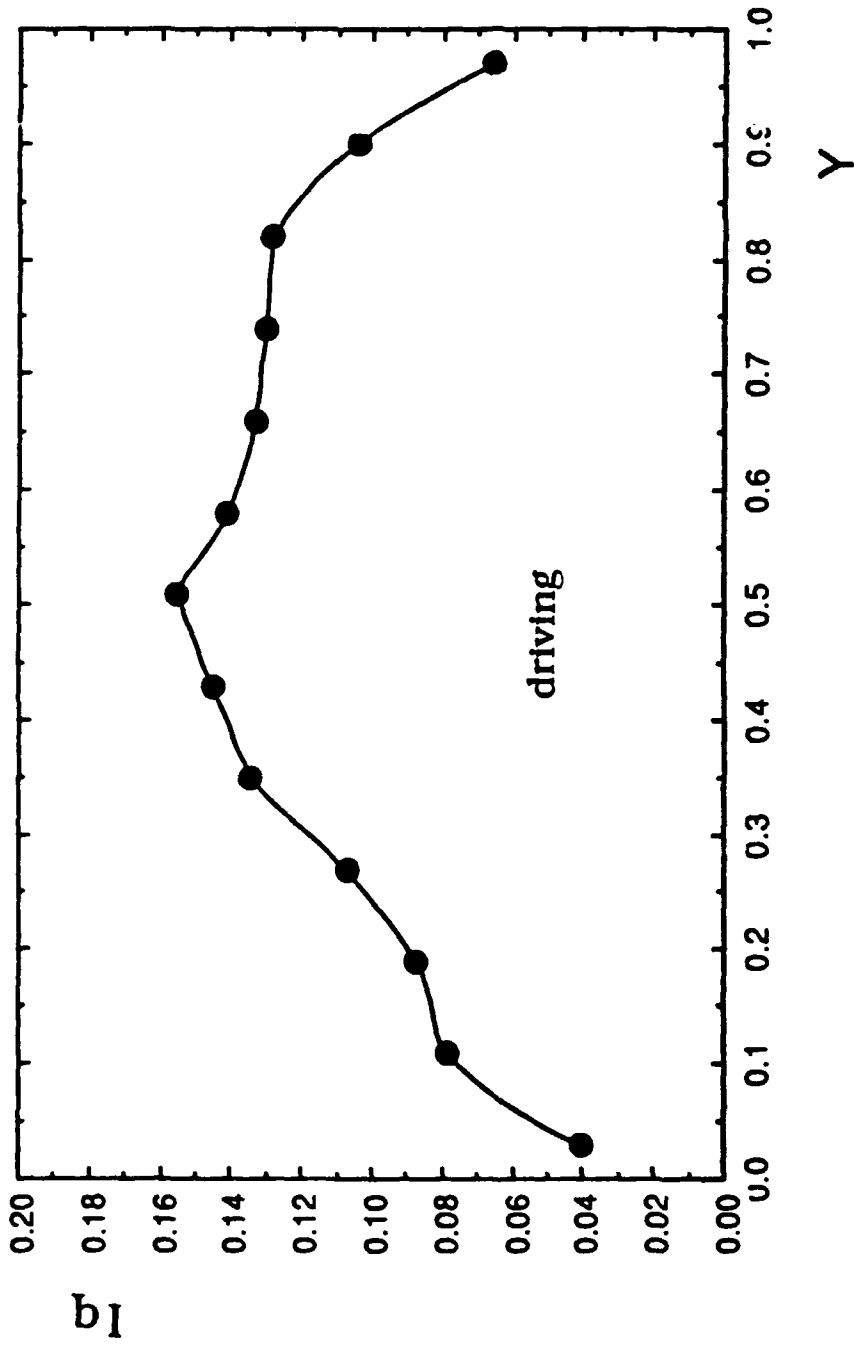
Figure 11. Variation of the Flame Driving/Damping along a Distance Normal to the Burner Surface of a Flame at a Pressure Antinode of a 400 Hz. Wave.
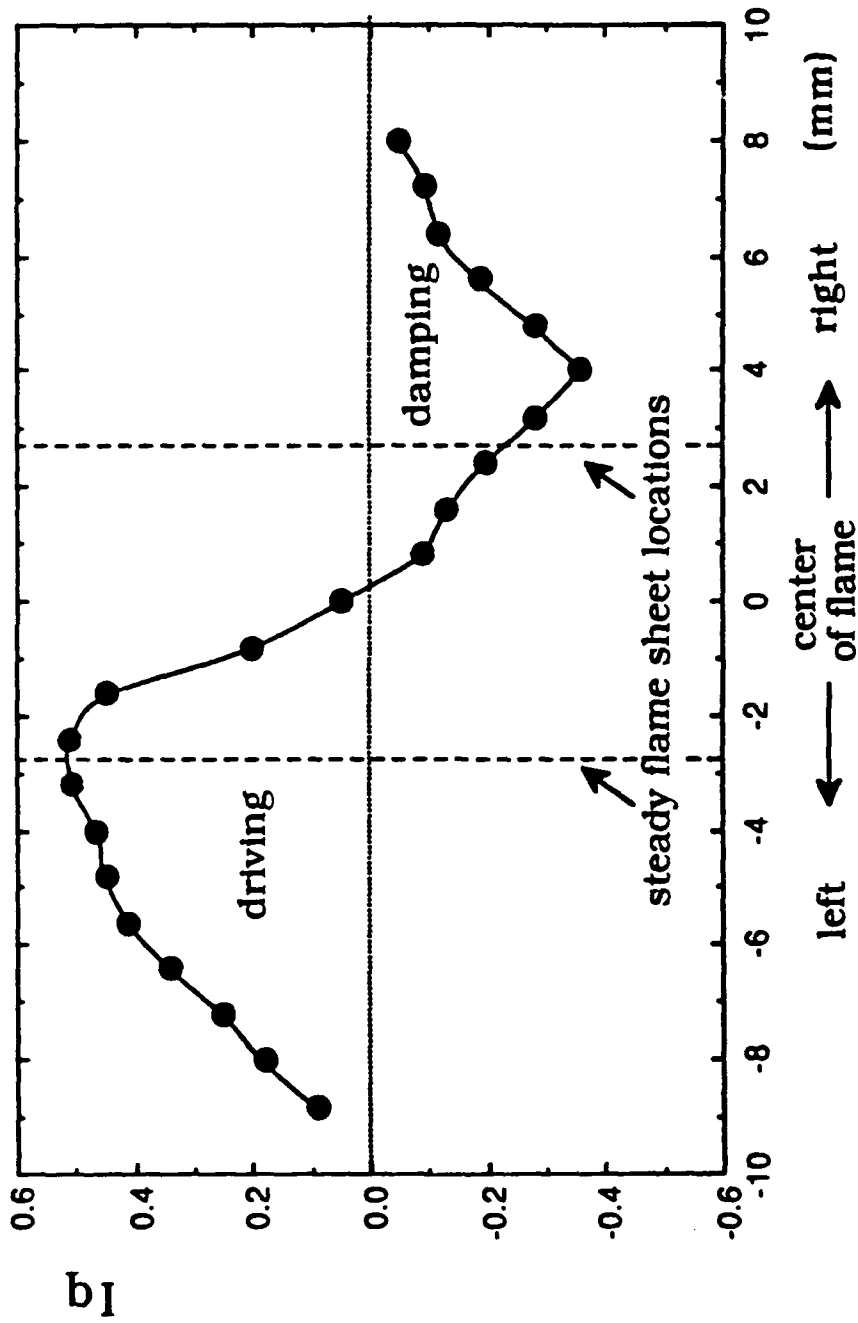
Figure 12. Axial Dependence of the Driving/Damping for a Flame Located at a Pressure Antinode of a 200 Hz. Wave.
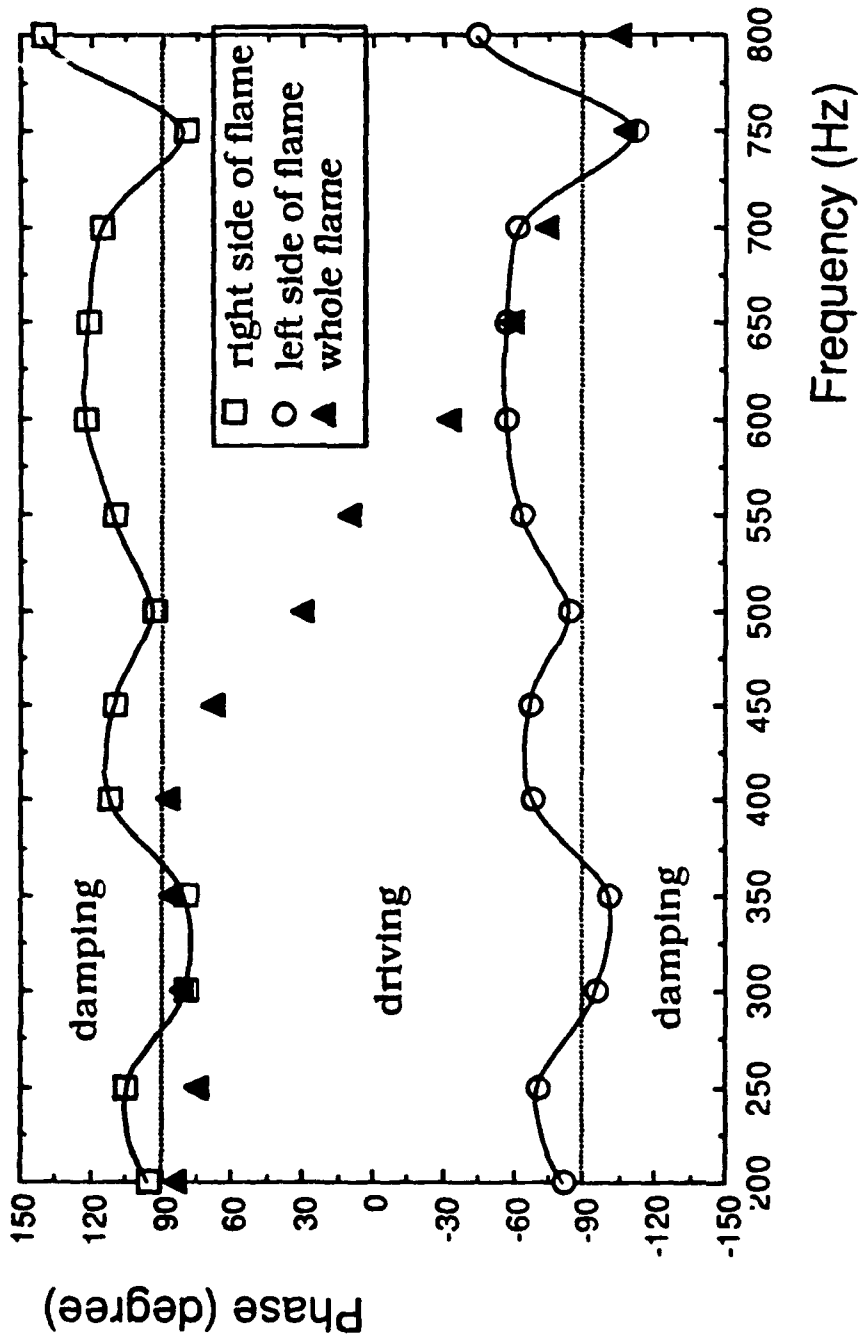
Figure 13. Frequency Dependence of the Phase Differences between the Radiation and Pressure Oscillations in Different Flame Regions of a Flame Located at a Pressure Node.
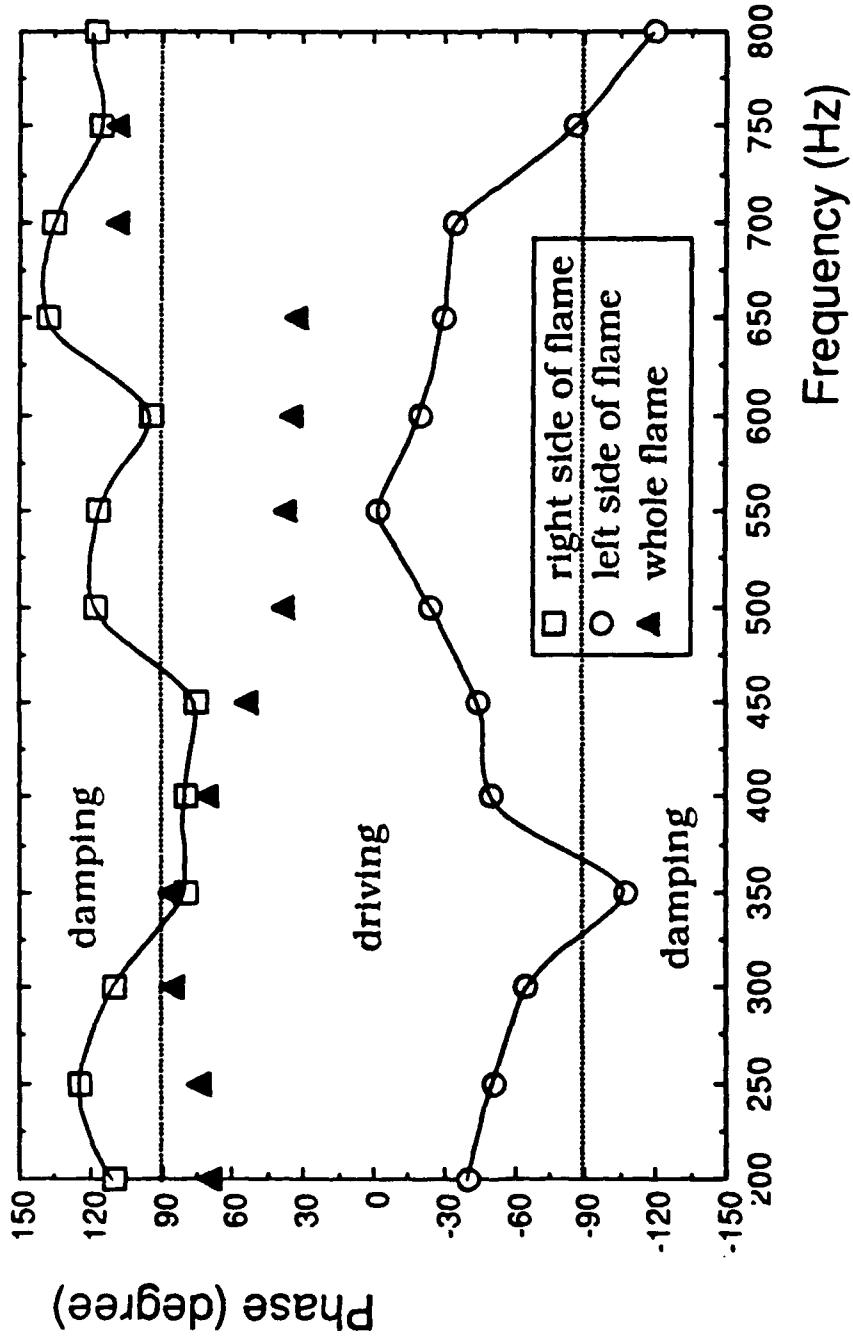
Figure 14. Frequency Dependence of the Phase Differences between the Radiation and Pressure Oscillations in Different Flame Regions of a Flame Located at a Pressure Antinode.
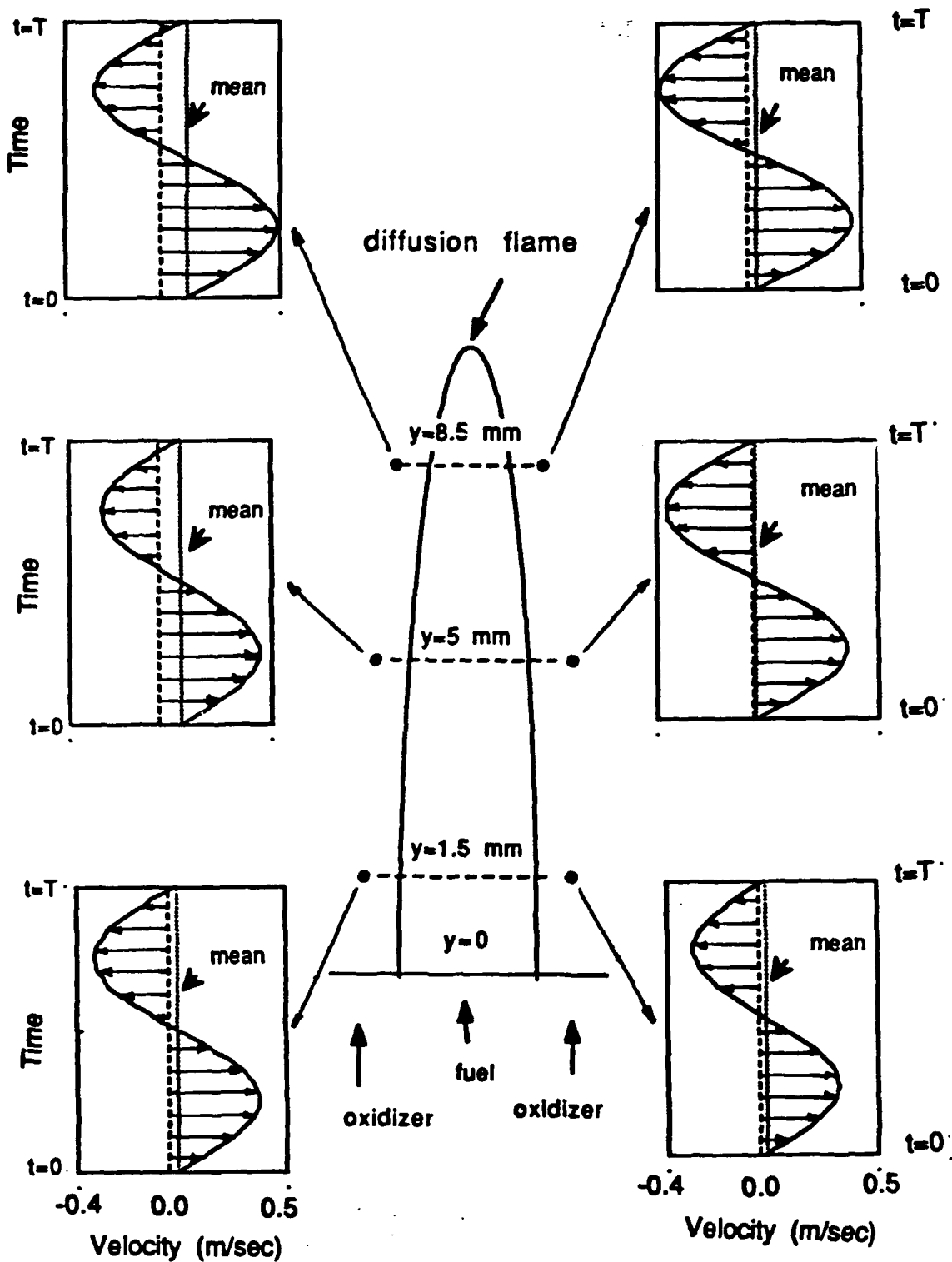
Figure 15. Time Trace of Axial Velocity on Both Oxidizer
Sides at Three Different Flame Locations of
a 200 Hz. Oscilaltion at a Pressure Node.
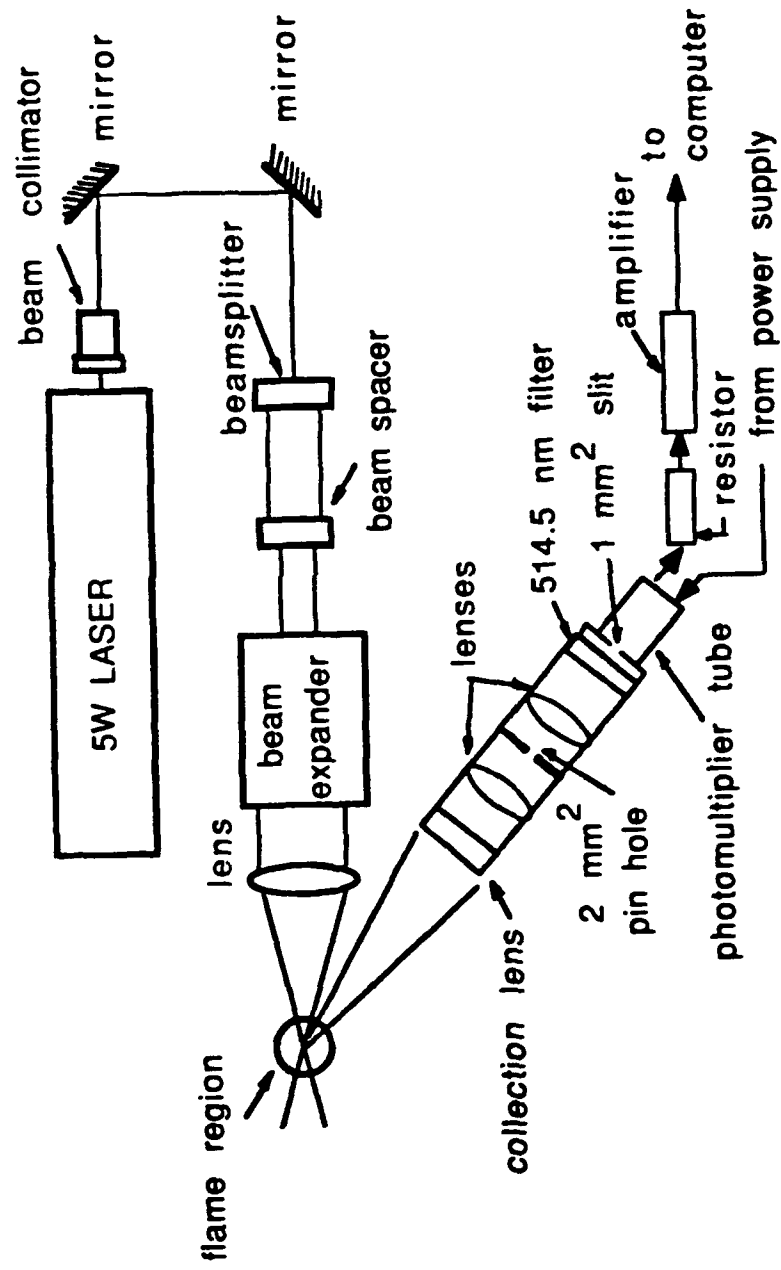
Figure 16. A Schematic of Experimental Setup for Rayleigh
Scattering Temperature Measurement
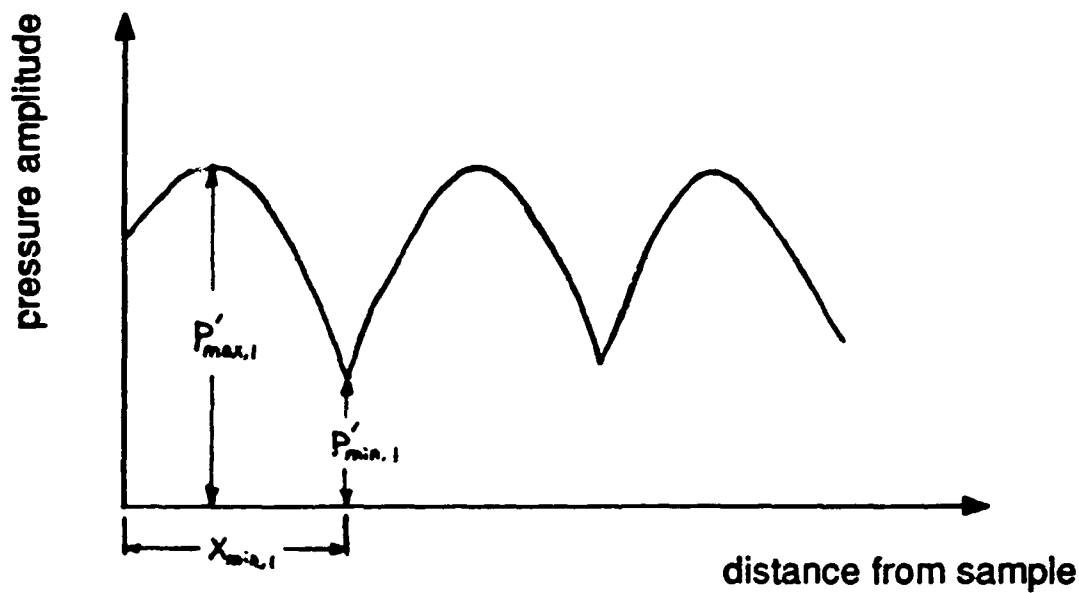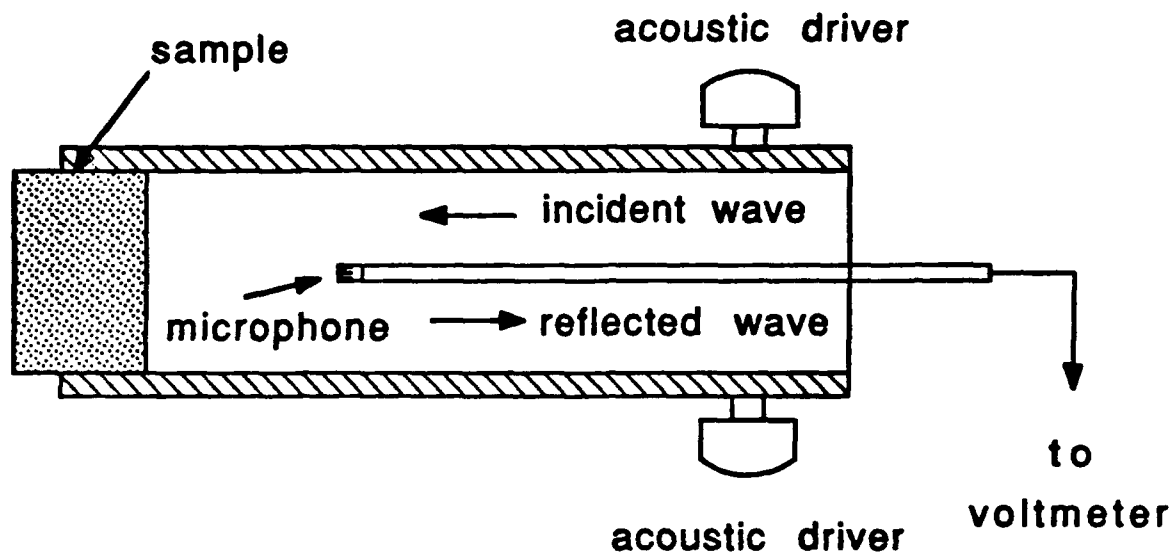
Standing Wave Pattern inside the Duct .

Figure 17. A Schematic of the Setup for Acoustic Amdittance Measurement.
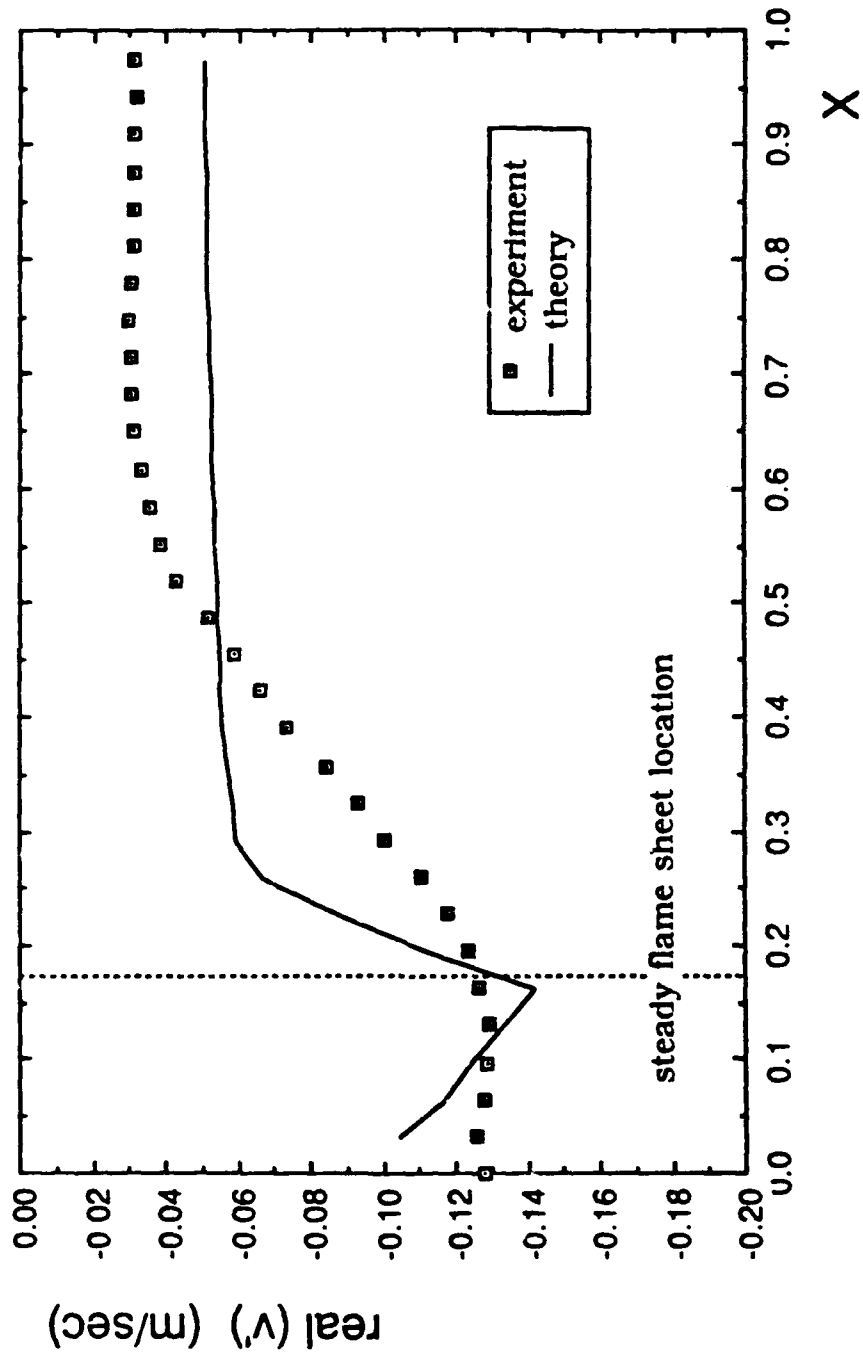
Figure 18. Measured and predicted Spatial Dependence of Real(v') at
$Y=Y_f$ of a 444 Hz. Acoustic Wave at a Pressure Antinode.
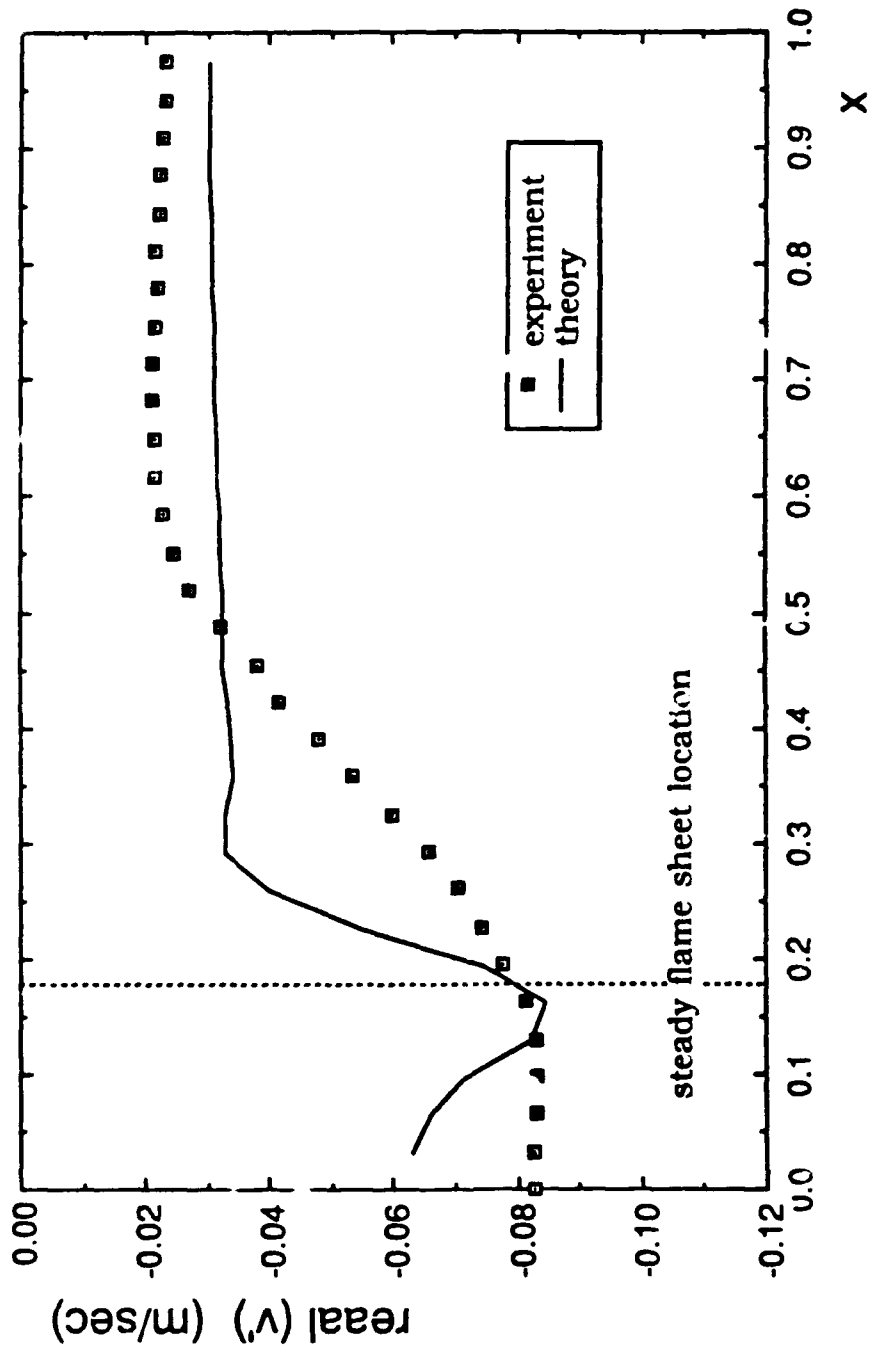
Figure 19. Measured and Predicted Spatial Dependence of Real(v') at Y=Y$_F$ of a 300 Hz. Acoustic Wave at a Pressure Antinode.
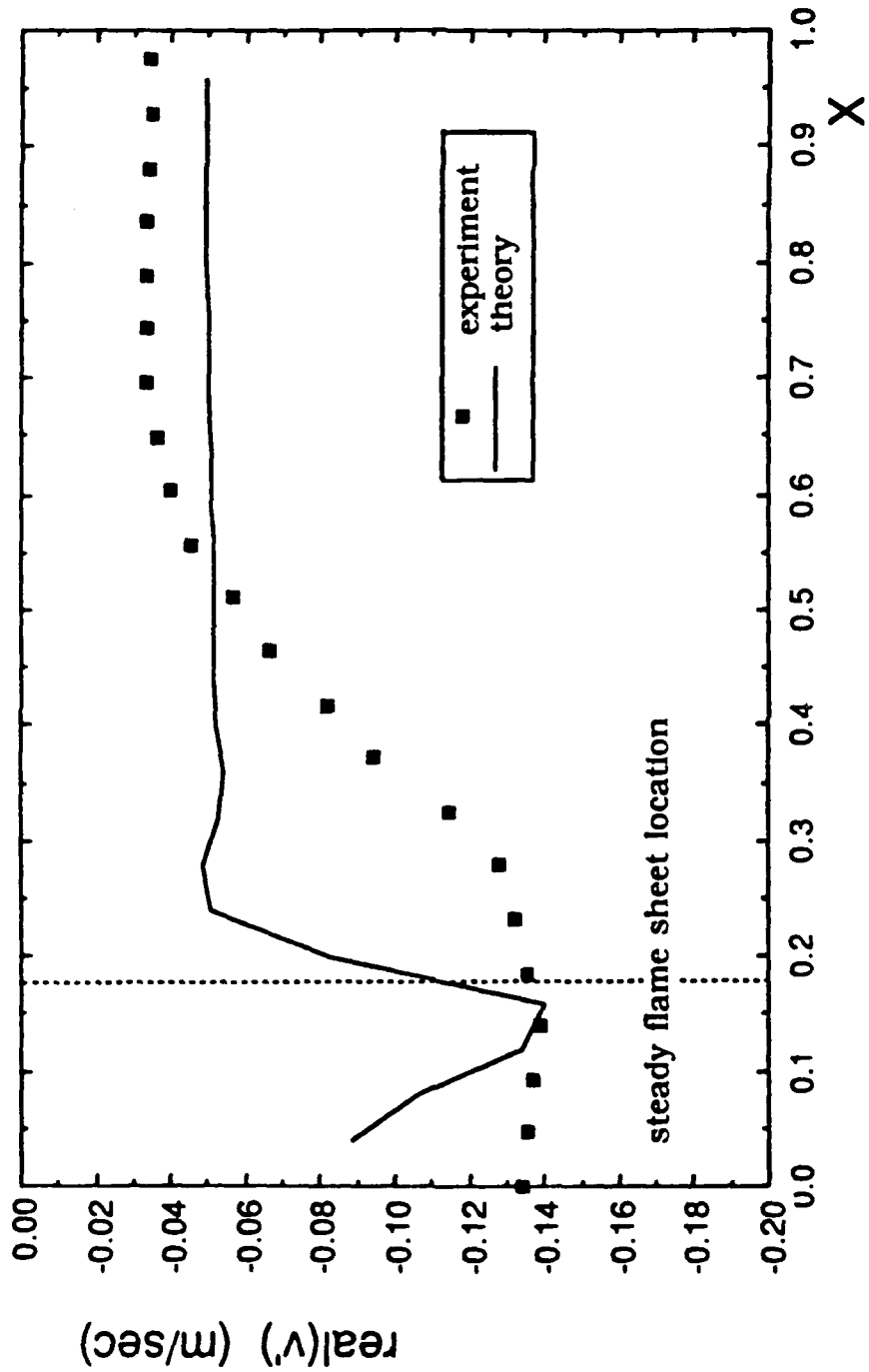
Figure 20. Measured and Predicted Spatial Dependence of Real(v') at Y=Y$_F$ of a 300 Hz. Acoustic Wave at a Pressure Antinode. (Larger amplitude of acoustic Excitation)

ACOUSTIC DRIVER

FLOW TURNING REGION
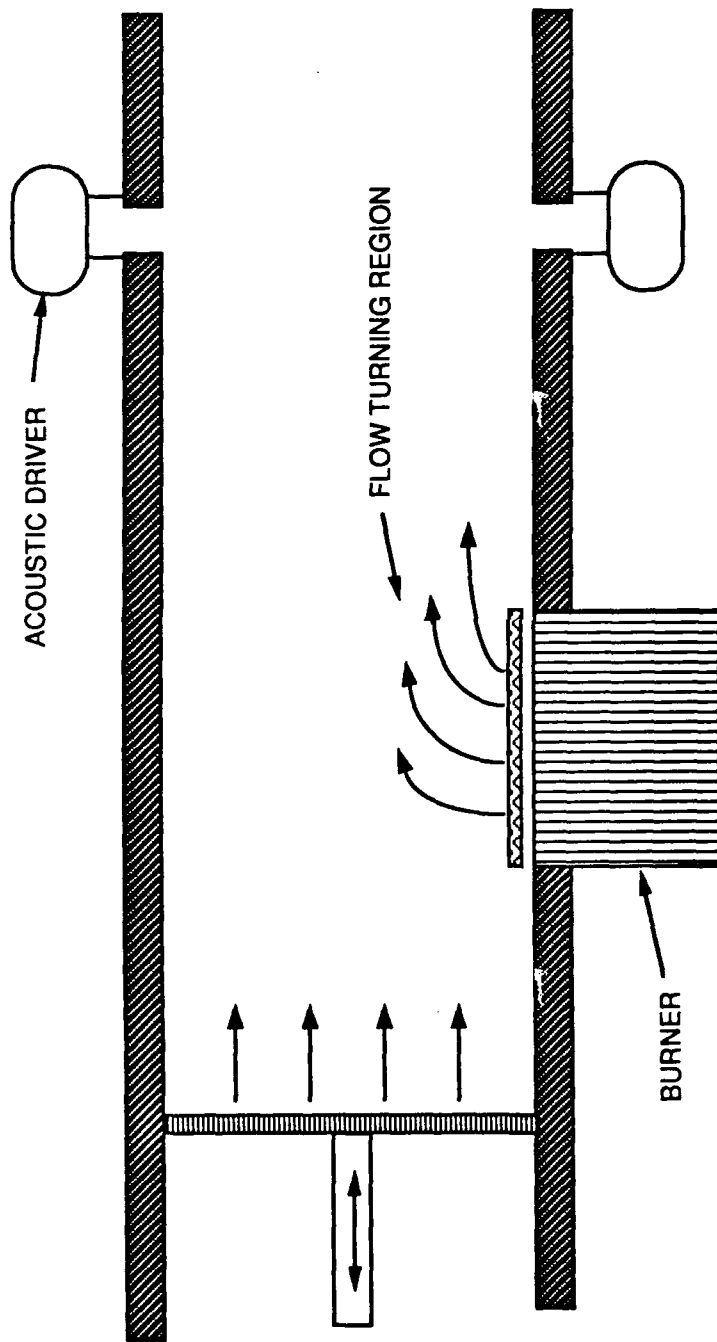
BURNER

Figure 21. A schematic of the experimental setup.
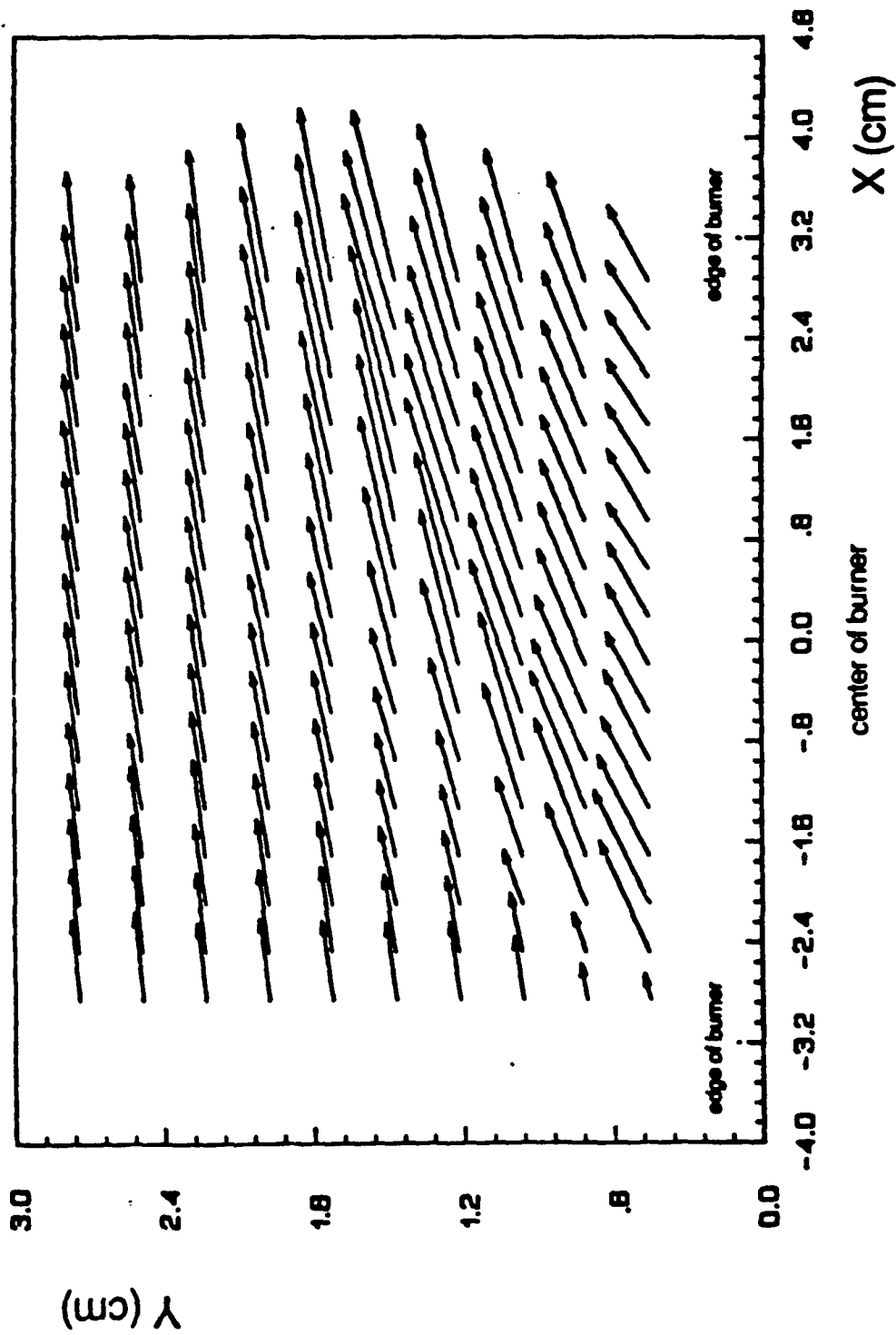
Figure 22. Vector diagram of the steady state velocity field above the burner in the experimental set-up. This example is for hot flow with a flame stabilized just above the burner surface.
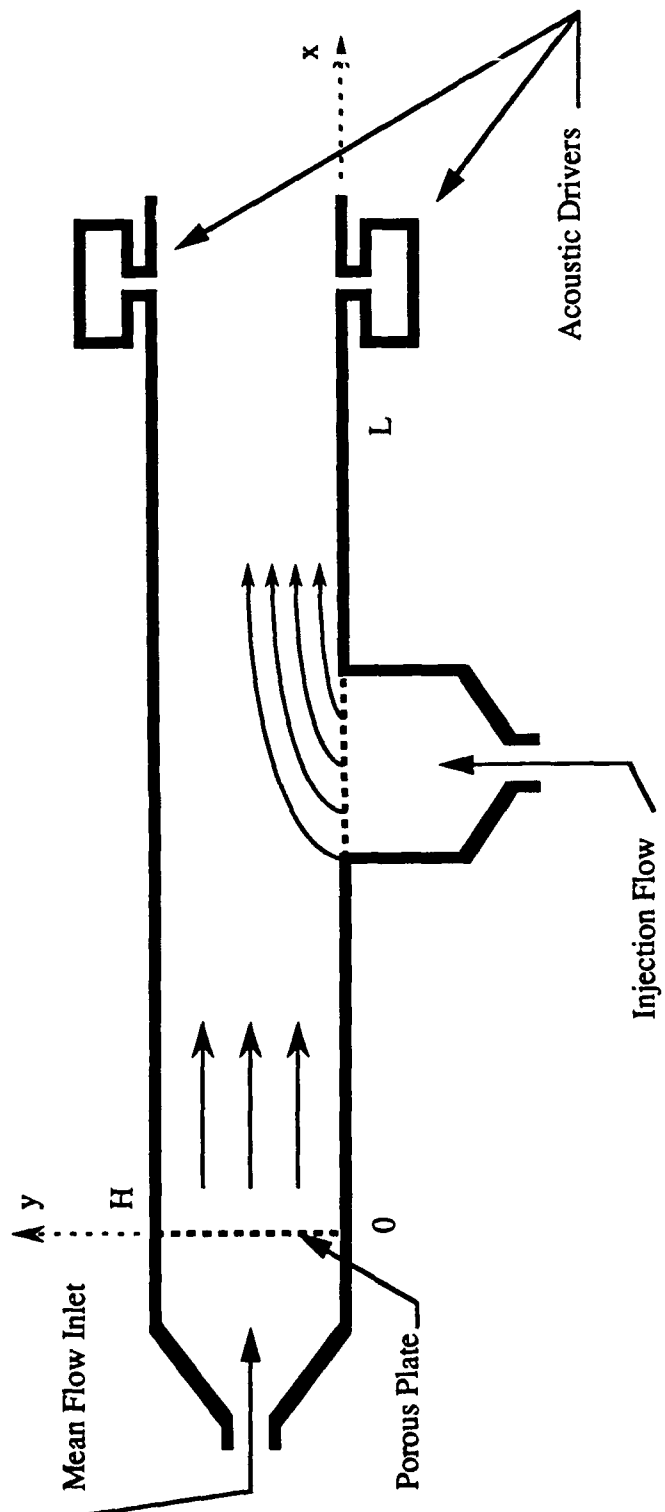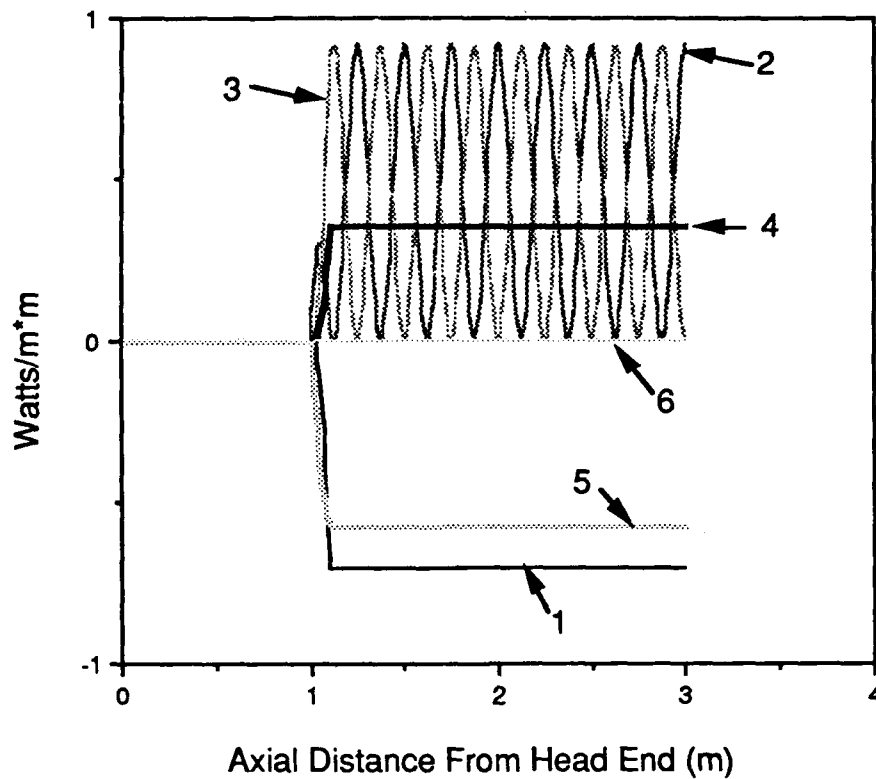
Figure 23. Schematic of the test section used in the numerical investigation of the magnitudes of the terms in the 1-dimensional acoustic stability equation. Walls and injectors are acoustically 'hard'.
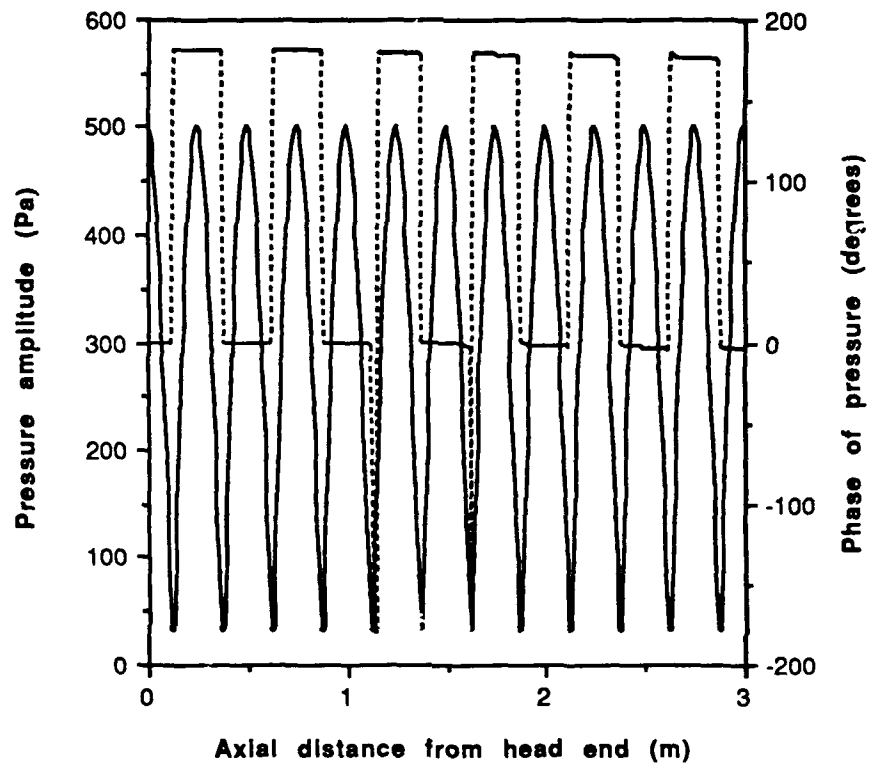
Figure 24. Numerically predicted amplitude and phase of the pressure oscillatio:. in a duct with side injection at a local pressure maxima. The phase is measured with respect to the pressure signal at x = 0. The injection occurs between x = 1.0 and x = 1.1.

$$1 = <\, p'\, u'\, >$$

$$4 = -\, <\int_0^x \frac{u'^2}{H}\, [\; m_{bo}\;]_0^H\, dx\; >$$

$$2 = <\frac{p'^2\, u_o}{\rho_o\, a^2}>$$

$$5 = <\int_0^x \frac{p'}{H}\, [\; \frac{m_b'}{\rho_o}\;]_0^H\, dx\; >$$

$$3 = <\, \rho_o\, u_o\, u'^2\, >$$

6 = The sum of above 5 terms.

Figure 25. Numerical prediction of the relevant terms on the right hand side of the 1-dimensional acoustic stability equation for a duct with side injection at 1.0m, in this case a pressure maxima. Term (4) is identified with the flow turning loss.
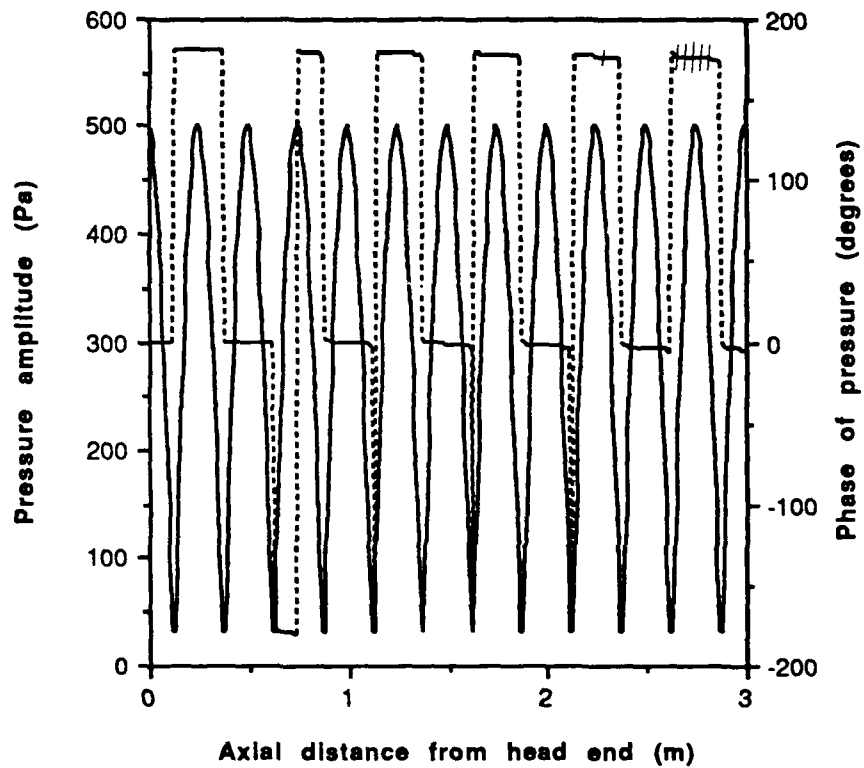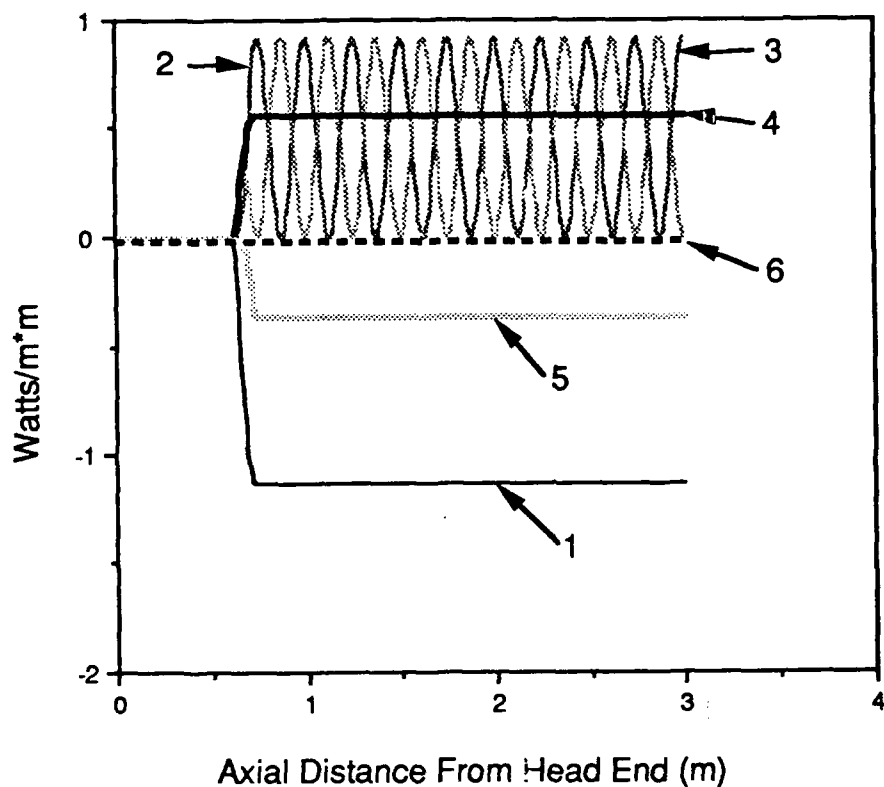
Figure 26. Numerically predicted amplitude and phase of
the pressure oscillation in a duct with side injection
at a local pressure minima. The phase is measured
with respect to the pressure signal at x = 0. The
injection occurs between x = 0.625 and x = 0.725.

$1 = < p' u' >$

$2 = <\dfrac{p'^2 u_o}{\rho_o a^2}>$

$3 = < \rho_o u_o u'^2 >$

$4 = - <\displaystyle\int_0^x \dfrac{u'^2}{H} [\, m_{bo} \,]_0^H \, dx >$

$5 = <\displaystyle\int_0^x \dfrac{p'}{H} [\, \dfrac{m_b'}{\rho_o} \,]_0^H \, dx >$

$6 =$ The sum of above 5 terms.

Figure 27. Numerical prediction of the relevant terms on the right hand side of the 1-dimensional acoustic stability equation for a duct with side injection at 0.625m, in this case a pressure minima. Term (4) is identified with the flow turning loss.